NASA Technical Memorandum 84528

Flutter Clearance of the Horizontal Tail of the Bellanca Skyrocket II Airplane

Rodney H. Ricketts, F. W. Cazier, Jr.,
and Moses G. Farmer

SEPTEMBER 1982

NASA

NASA Technical Memorandum 84528

Flutter Clearance of the Horizontal Tail of the Bellanca Skyrocket II Airplane

Rodney H. Ricketts, F. W. Cazier, Jr.,
and Moses G. Farmer
Langley Research Center
Hampton, Virginia

National Aeronautics
and Space Administration

**Scientific and Technical
Information Branch**

1982

Use of trade names or names of manufacturers in this report does not constitute an official endorsement of such products or manufacturers, either expressed or implied, by the National Aeronautics and Space Administration.

SUMMARY

The Skyrocket II is an all-composite-constructed experimental prototype airplane built by Bellanca Aircraft Engineering, Incorporated. A flutter-clearance program was conducted on the horizontal tail so that the airplane could be safely flown to acquire natural-laminar-flow aerodynamic data. A ground-vibration test was conducted on the tail to acquire both symmetric and antisymmetric mode shapes, frequency, and generalized mass data. These were used in flutter analyses that employ subsonic lifting-surface theory to calculate horizontal-tail flutter boundaries. The symmetric flutter boundary was more critical than the antisymmetric flutter boundary and was sensitive to the values of structural damping coefficient used in the analyses. Flight tests were made to acquire flutter data which were then analyzed with the Peak-Hold and Randomdec subcritical-response techniques to predict flutter speeds for two different modes. One flutter speed predicted from flight data compares favorably with the analytical results. However, the final flutter-clearance placard speed was based on the second flutter speed predicted from flight data. This placard did not restrict the acquisition of the natural-laminar-flow aerodynamic data.

INTRODUCTION

The Skyrocket II is a single-engine, six-place, low-wing, experimental prototype general aviation airplane which was constructed of fiberglass and aluminum honeycomb-composite sandwich materials. A photograph and a three-view drawing of the airplane are shown in figures 1 and 2, respectively. The airplane was built by Bellanca Aircraft Engineering, Incorporated, and was first flown in 1975. Because of its smooth skins and low-protuberance drag, the airplane proved to be fast enough to acquire world speed records in several classes.

The Skyrocket II was not flown again until early 1981 when NASA became interested in studying the natural laminar flow over the smooth wing surfaces. (See ref. 1.) Because the airplane had been stored outside during the period from 1976 to 1981, there was concern that the structure may have suffered degradation due to exposure to sunlight and moisture. A strip-theory flutter analysis conducted by the manufacturer in 1975 predicted that the horizontal tail was the most critical lifting surface and that its flutter boundary was coincident with the velocities achieved during the speed-record flights. Although this analysis proved to be conservative (because no flutter was observed during the flights), structural degradation could possibly remove any margin that existed and move the flutter boundary into the flight envelope.

A review in 1981 of the fundamental horizontal-tail frequencies revealed substantial differences from the 1975 data in the elevator rotation mode and to a lesser extent in the stabilizer bending mode. Because of these differences a more extensive ground-vibration test of the horizontal tail was performed. The measured modal data were used in a new, independent flutter analysis. A flutter-clearance program was then conducted on the horizontal tail to define a flight envelope in which the natural-laminar-flow data could be safely acquired. The limited instrumentation and flight-data recording capability used in this test were consistent with the program

goals and estimated flutter risk. More extensive instrumentation and analyses would normally be employed, including telemetry, real-time monitoring from the ground, and additional accelerometers.

The present paper describes the details of this flutter-clearance program. Both the ground-vibration test results and analytical flutter results are presented. Subcritical-response data acquired during flight tests are also presented and compared with the analytical predictions.

SYMBOLS

A	amplitude of response peak
c	chord, in.
f	frequency, Hz
Δf	incremental frequency, Hz
g	structural damping coefficient ($g = 2\gamma$)
h	pressure altitude, ft
M	Mach number
m_g	generalized mass, slugs
V	velocity, mph
x	streamwise dimension, in.
y	spanwise dimension, in.
z(i)	vertical displacement of ith mode
γ	viscous damping ratio

Abbreviations:

EAS	equivalent airspeed
GVT	ground-vibration test
IAS	indicated airspeed
rms	root mean square
V-f	velocity-frequency
V-g	velocity-damping

DESCRIPTION OF HORIZONTAL TAIL

The horizontal-tail geometry is shown in figure 2. The tail is composed of a stabilizer and a full-span elevator. The stabilizer can be moved by an electric motor to trim the airplane statically. It is constructed of fiberglass and aluminum honeycomb-composite sandwich skins attached to aluminum spars. The elevator is controlled with cables that are stretched to a tension of 15 lb. It is constructed of fiberglass and foam and is balanced with mass at the tips.

GROUND TEST

A ground-vibration test (GVT) was conducted to measure the mode shapes, natural frequencies, and generalized masses of the horizontal tail.

Procedure and Apparatus

During the GVT the airplane was supported by the landing gear with the tires deflated to low pressures. This minimized the influence of the tire mode on the structural modes. The structural modes were excited by two electromagnetic shakers capable of an output of 10 lb of force. The shakers were used to excite both the symmetric and antisymmetric modes, and they were positioned against the lower surface of the tail. To identify natural frequencies, logarithmic frequency sweeps were made with a sweep oscillator to drive the shakers. The resulting structural response was measured by accelerometers fixed to the tail and was analyzed by a SD330A Spectral Dynamics spectrascope real-time analyzer. The structural modes are indicated by the peaks on the analyzer display. Each mode was then tuned in and its shape was defined by measuring the acceleration at each of 42 grid points on the tail with a roving accelerometer while the shaker input force was held constant. The grid-point locations are shown in figure 3 and are listed in table I. The structural damping for each mode was determined by first exciting the mode, then physically removing the shaker from the tail surface, and finally measuring the logarithmic decrement of the resultant decaying signal. Generalized masses were calculated from measured variations in frequency that were the result of the addition of small masses to the structure. This method is described in detail in reference 2.

Results

During the ground-vibration survey, results for five symmetric and three antisymmetric modes with natural frequencies up to 50 Hz were obtained. The symmetric results are presented in table II and figure 4. For these results, the modal frequencies, generalized masses, and structural damping are given in table II(a). Modes 1, 4, and 5 are primarily stabilizer modes, whereas modes 2 and 3 are elevator modes. A range of generalized masses was determined from measurements with masses added at several locations. In addition, the frequencies of the modes as they were measured in 1975 are presented for comparison with the current measurements. Two elevator-rotation modes (modes 2 and 3) were currently measured, whereas only one mode was measured in 1975. The modal displacements at each grid point are given in table II(b). The mode shapes are presented graphically in figure 4 as node-line

plots and oblique-projection figures. The corresponding antisymmetric results are given in table III and figure 5. Mode 1 is a stabilizer mode, whereas modes 2 and 3 are elevator modes.

FLUTTER ANALYSIS

Symmetric- and antisymmetric-flutter analyses of the horizontal tail were performed with the measured modes, frequencies, and generalized masses. All velocities in this section are expressed as equivalent airspeed (EAS).

Methods and Procedures

Unsteady aerodynamics for use in the flutter analysis were calculated with the linear lifting-surface theory described in reference 3. The theory is a kernel-function approach which allows control surfaces, such as the elevator, to be present in the analysis of an isolated lifting surface. In this implementation of the theory, a surface spline is used to interpolate the measured mode shapes in order to calculate displacements at the downwash collocation points of the analysis. Thirty-six collocation points, six chordwise points at each of the six spanwise stations, were used for these analyses.

A modified version of the FAST routine described in reference 4 was used to solve the flutter eigenvalue problem and to plot the results. The routine uses the traditional incremental damping approach (V-g method) to solve for the flutter velocity. The results appear as damping plotted against velocity and frequency plotted against velocity for each altitude and Mach number calculation. In addition, the flutter eigenvector is calculated for each flutter-speed crossing.

Analyses were performed for both symmetric and antisymmetric modes. For the symmetric-flutter analysis, calculations with incremental variations in the structural damping, measured frequencies, and measured generalized masses were performed to determine the sensitivity of the flutter speed to these parameters.

Results

Symmetric-flutter analyses.- Symmetric-flutter analyses were performed at Mach numbers of 0.3, 0.4, 0.5, and 0.6. Examples of the velocity-damping and velocity-frequency (V-f) results are shown in figure 6. For these results, the analysis Mach number is 0.3, altitude is 10 000 ft, and values of structural damping are zero. The flutter eigenvector given in table IV(a) for the critical mode shows that the symmetric flutter mode is primarily composed of mode 5 with some coupling present from other modes.

The root of the critical flutter mode has a low gradient (dg/dV) at the crossing, as shown in the V-g plot in figure 6. This indicates that the flutter velocity is very sensitive to the amount of structural damping used in the analysis. For this reason, the analyses were repeated for a structural-damping value of 0.02 for each measured mode shape. (The actual structural damping in each measured mode is very near or greater than the value of 0.02. See table II(a).)

The resulting symmetric flutter boundary for the two cases of structural damping (0 and 0.02) are presented in figure 7. As indicated earlier, the addition of struc-

tural damping to the modes substantially affects the calculated results. The flutter velocity is increased by approximately 30 percent throughout the altitude range. The flutter frequency is approximately 45 Hz along the boundary for each case.

A flutter analysis was performed by the manufacturer in 1975 with strip theory, measured modes, and frequencies. The results of this analysis with zero structural damping showed that the symmetric elevator-rotation mode became unstable at 213 mph. (The elevator rotation mode corresponds to modes 2 and 3 in the present analysis.) This flutter speed agrees somewhat with the present zero-structural-damping analysis, even though the mode that becomes unstable is not the same. The flutter speed calculated in the 1975 analysis is also shown in figure 7.

To determine the sensitivity of the flutter speed to some additional parametric variations in the present analysis, measured frequencies and generalized masses were incremented for each mode separately. The results of these calculations are shown as bar graphs in figure 8.

In figure 8(a) variations in flutter speed are shown for analyses in which the GVT frequencies were incremented ±1.0 Hz for each mode individually. In figure 8(b) variations in flutter speed are shown for analyses in which the GVT generalized masses are incremented from the lower measured value (nominal) to the upper measured value. (See table II(a).) Although the variations in flutter speed are small for both sets of analyses, the results do show that the flutter velocity is most sensitive to changes in measured values (both frequency and generalized mass) for mode 5. This is not surprising because this mode was a major contribution to the flutter-mode shape. (See table IV(a).)

Antisymmetric-flutter analysis.- An antisymmetric-flutter analysis was performed at a Mach number of 0.3. An example of these results is shown in the V-g and V-f plots presented in figure 9. For these results, the analysis altitude is 10 000 ft and the structural-damping value for each mode is zero. The flutter eigenvector given in table IV(b) for the critical mode shows that the antisymmetric flutter mode is composed primarily of mode 3 with some coupling with the other values.

The results of this analysis show that the antisymmetric-flutter velocity is considerably higher than the symmetric-flutter velocity. Therefore, additional analyses in which Mach number, damping, frequency, and generalized mass are varied (as with the symmetric-flutter analysis) were not performed.

FLIGHT TEST

The third and final segment of the flutter-clearance program was the flight test of the airplane. All flight-test velocities in this section are given as indicated airspeed (IAS). For incompressible flow, which is an appropriate assumption of this study, indicated airspeed and equivalent airspeed (from the analysis) are very nearly the same. (Calibrated airspeeds for this airplane are within ±2 percent of the indicated airspeeds presented here.)

Procedures and Equipment

A series of eight flights was made to gather subcritical data on the horizontal tail at small velocity increments and to expand gradually and safely the flight envelope of the airplane after post-flight analysis of the data. During each flight,

data were gathered at three to four velocities which were incremented by 10 mph. Each successive flight duplicated previous data points and expanded the flight envelope by no more than 10 mph. A chart is presented in figure 10 which shows the velocity ranges for the data acquired and illustrates the envelope-expansion procedure. A chase airplane was present during each flight so that the pilot could observe any motions of the horizontal tail or other components of the flight-test airplane.

Instrumentation onboard the airplane for acquiring the structural-response data included two accelerometers, signal-conditioning equipment and a magnetic tape recorder. The accelerometers were attached to the surface of the tail at the right tip as shown in figure 11 - one on the upper surface of the stabilizer and the other on the lower surface of the elevator. The signal-conditioning equipment was supplied by Ohio State University and used 115 V, 60-Hz current derived from the 28 V, dc power of the airplane. The tape recorder was powered by internal batteries. In addition to the accelerometer signals, flight conditions and data-point identification given by the pilot were recorded with an open microphone.

During each flight the following procedure was used to acquire the data. The airplane was first flown to an altitude of approximately 12 000 ft and was then stabilized at the initial test velocity. The engine speed was set at 2900 rpm. Data were recorded for a period of 2 min at this velocity. The velocity was then increased to the next test point by holding the power and engine speed constant and putting the airplane into a slight dive. With the velocity stabilized, data were again recorded for 2 min. This procedure was continued until either all the test points were completed or until an altitude of 8000 ft was reached. If the test points were incomplete, the airplane was flown to a higher altitude again to continue testing. The nominal flight-test altitude was 10 000 ft. During the data recording for all test points, the pilot tried to ensure that a relatively constant level of atmospheric turbulence was present. Because the airplane was not equipped with any turbulence-measuring instruments, this was a subjective determination made by the pilot. Each flight lasted approximately 1 hr.

After each flight the data were analyzed by subcritical response methods to indicate any impending flutter conditions. The time required to analyze the data averaged about 3 hr. Permission to proceed with each additional flight was judged on the results of the predictions of the subcritical-response methods.

Subcritical-Response Methods

Two methods of subcritical-response data analysis were used to predict flutter from the test data. These are the Peak-Hold and Randomdec methods which are described in detail in reference 5. Both methods assume that ambient random inputs excite the structural modes of interest. A general explanation of each method is provided here. Although other subcritical-response methods (see ref. 6) employ forced excitations through the use of aerodynamic vanes or mass shakers, ambient excitation was chosen because of expediency and simplicity. The use of ambient excitation methods, however, can sometimes lead to scatter in the results because the turbulence level and waveform are an unmeasurable, and often variable, quantity.

Peak-Hold.- In the Peak-Hold method, the root-mean-square (rms) response of an accelerometer signal is measured as a function of frequency with a real-time analyzer. Amplitude peaks are monitored for growth as velocity increases. The rise in a peak is a possible indication of impending flutter. The rise could also be due

to an increase in the level of the forcing function which is driving the signal. Flutter occurs at the velocity where the amplitude of the peak becomes infinite, or, in other words, where the inverse amplitude is zero. Therefore, the inverse amplitude data are plotted against velocity, and then a curve is faired through the data points and is extrapolated to a zero crossing. The velocity where the inverse amplitude is zero is the projected flutter speed. Both a Hewlett-Packard 5420A digital signal analyzer and the previously mentioned Spectral Dynamics real-time analyzer were used to reduce the data for the Peak-Hold method. This method was used to analyze the data after each flight.

Randomdec.- On some occasions, the Randomdec method was used to check the Peak-Hold results. In the Randomdec method, the data are first filtered with a digital band-pass filter that has a bandwidth of 3 Hz and a center frequency at a response peak, and then they are ensemble-averaged to produce a signature. Viscous damping ratios are calculated from the logarithmic decay of the signature. A Xerox Sigma 5 computer was used to implement this method.

Results

The results of the flight test include Peak-Hold frequency-response spectra and inverse amplitudes, in addition to Randomdec signatures and damping ratios.

Typical Peak-Hold frequency-response spectra are presented in figure 12. The data were acquired with the elevator accelerometer (fig. 12(a)) and the stabilizer accelerometer (fig. 12(b)) at an IAS velocity of 220 mph. In these figures several frequencies from extraneous signals are shown, which hampered the analysis of the data. These extraneous signals were produced by the following: the engine speed of 48 Hz (2900 rpm); a subharmonic of the engine speed at 24 Hz; the propeller speed of 32 Hz which occurred because of a 2:3 gearing ratio between the propeller and the engine; and, occasionally, a 60-Hz noise arising from the data-reduction equipment setup. An additional signal at 96 Hz (not shown) came from the magneto whose frequency was twice that of the engine. This signal entered the signal-conditioning equipment and dominated the time-history data.

Frequencies of importance in figure 12 include the following: the predicted analytical-flutter mode at 45 Hz, a signal of unknown origin at 27 Hz, and a harmonic of the unknown signal at 54 Hz which had a peak amplitude that was proportional to that of the 27-Hz peak. Two possible sources of the 27-Hz signal and the harmonic are discussed in the following two paragraphs. Although the sources of these two signals are not known, they were treated as possible flutter candidates.

(1) An additional piece of electrical equipment onboard the airplane could be the source of this signal. Because the signal-conditioning equipment was connected to airplane power, the accelerometers were susceptible to many sources of noise as discussed previously. However, this type of signal is not normally a function of airspeed as indicated by the data.

(2) A more plausible explanation for the source of the signal is the forced response of the horizontal tail. During the flights the left main landing-gear door was observed to vibrate at speeds above 180 mph. Pressure differentials over the door caused it to open partially, allowing the door to vibrate. The door vibration (whose frequency was not determined) either could have been transmitted through the structure (the pilot reported feeling a vibration in his seat) or could have excited the airstream which impinged on the tail. (Harmonics are known to exist in unsteady

airflows.) Thus, the tail could have been forced to vibrate in its 27-Hz antisymmetric GVT mode. Antisymmetric tail vibration is further supported because only one door was vibrating and, therefore, producing an asymmetric condition.

In figure 13 the Peak-Hold results from flights 5 to 8 (see fig. 10) are presented for two frequency peaks - namely, 27 to 28 Hz and 45 to 46 Hz - from the elevator-accelerometer data. (The 54-Hz data are not shown because of their similarity to the 27-Hz data.) For both sets of peaks the frequency generally decreases as the velocity increases. A least-squares fit of the data was used for extrapolation to an inverse peak amplitude of zero for the flutter prediction. A flutter speed of 347 mph is predicted for the 45-Hz data, whereas the 27-Hz data yield a predicted flutter speed of 237 mph.

Randomdec signatures for response at 27 and 45 Hz are presented in figure 14. The flight data are the same as those used in the Peak-Hold frequency spectrum (fig. 12(a)) acquired for the elevator accelerometer at 220 mph. The signatures were developed from 30 sec of flight data which were sampled at 300 samples per second. The damping ratio measured from the 27-Hz signature (fig. 14(a)) is the very low value of 0.002. The damping ratio measured from the 45-Hz signature (fig. 14(b)) is higher at 0.010. The quality of the signature in both cases is good in that the signature is smooth, decays logarithmically, and contains no beats.

The Randomdec damping results from flights 5 and 8 are presented in figure 15 for the 27- and 45-Hz modes. Although some scatter exists in the data, these results agree favorably with those from the Peak-Hold method. (See fig. 13.) The 27-Hz mode becomes very lowly damped near 220 mph, whereas the damping level of the 45-Hz mode remains relatively constant to 220 mph. Extrapolation of the 27-Hz data gives a flutter speed of 222 mph. Because of the scatter in the 45-Hz results, extrapolation to a flutter point for this mode is not generally feasible for this limited set of data.

DISCUSSION OF RESULTS

GVT and Theoretical Results

A comparison of the current ground-vibration test results (GVT) and those measured in 1975 (see tables II(a) and III(a)) generally shows that the stabilizer frequencies were lower and the elevator frequencies were higher for the present measurements. Specifically, the symmetric stabilizer bending-mode frequency dropped by 14 percent and the symmetric elevator-rotation-mode frequencies increased from 52 to 72 percent. Although the reasons for these large differences are not known, these results do have a bearing on the comparison of the current flutter results and those obtained in 1975. As previously stated, different modes couple in each analysis to form the flutter mode. In the 1975 analysis, the elevator-rotation mode was the primary participant. However, in the current analysis this mode did not yield a flutter instability. A possible explanation for the lack of this instability is given in reference 7. It is shown that flutter of the elevator is dependent upon the control static unbalance and upon the ratio of the frequencies of the elevator rotation and the stabilizer bending modes. As this ratio increases, for constant unbalance, the flutter speed gradually decreases until the instability abruptly disappears. The current frequency ratio (greater than 2.0) is in the range where this type of instability should not exist.

Flight Test and Theoretical Results

The Peak-Hold results at 45 to 46 Hz (see fig. 13) from the analysis of the measured flight-test data are in fair agreement with the theoretical predictions. Linear projection of the data predicts a flutter speed of 347 mph, or a speed 12 percent higher than the symmetric theoretical prediction with structural-damping values of 0.02. (The analysis is conservative in predicting the flutter speed.) The use of larger values of structural damping to represent more closely the damping of the actual structure (see table II) would increase the theoretical flutter speed and remove some of the conservatism of the analysis. Linearly extrapolating the frequencies of the data (ranging from 46 Hz at the low velocity to 45 Hz at the high velocity) yields a frequency of 43 Hz at flutter. This is within ± 2 percent of the theoretical flutter frequency.

The Peak-Hold results at 27 to 28 Hz (see fig. 13), however, do not agree with either symmetric or antisymmetric theoretical predictions. Both the flutter speed and the flutter frequency derived from extrapolations of the subcritical data are far removed from the theoretical values. This disagreement would be easily explained if the source of the signal was not related to flutter of the tail. However, because of the trend of the results and because the source has not been identified, this response must be treated as a flutter response for flight-safety purposes.

The flight conditions (altitude and velocity) covered during this flight test are shown in figure 16. The projected flutter point for the subcritical-response data at 27 to 28 Hz is also shown in this figure. To allow for airplane overspeeds and gust velocities during the wing natural-laminar-flow studies, it was necessary, for safety reasons, to placard the airplane flight envelope. The limit airspeed was chosen as 205 mph to allow a 15-percent margin in velocity. This 205-mph placard still allowed the required natural-laminar-flow measurements to be made. Therefore, it was not necessary to define the mode at 27 to 28 Hz further or to attempt to expand the flight envelope further.

As previously explained, many extraneous airplane signals appeared in the data measured on the accelerometers. The signal-conditioning equipment was picking up this "noise" from the airplane power. This problem could possibly be alleviated by supplying the signal-conditioning equipment with a power source other than airplane power.

CONCLUSIONS

A flutter-clearance program was satisfactorily conducted on the horizontal tail of the Bellanca Skyrocket II airplane to define a flight envelope in which natural-laminar-flow data could be safely acquired. The following conclusions were made during the clearance program:

1. A recent ground-vibration test of the horizontal-tail modes of the Skyrocket II airplane showed that the natural frequencies were different from those measured in 1975. The symmetric stabilizer frequencies were lower by as much as 14 percent. The symmetric elevator-rotation frequencies were higher by as much as 72 percent. The reasons for these differences are not known. However, because of these differences, further analysis and flight tests were required to insure a safe flight envelope.

2. Linear lifting-surface theory was used to predict the subsonic flutter speeds of the horizontal tail consisting of a combination of a stabilizer and a full-span

elevator. The flutter velocity was sensitive to structural damping of the modes used in the analysis. The zero-damping flutter speeds agreed fairly well with the flutter speed calculated in 1975 with a strip-theory analysis, even though different modes coupled to produce flutter at a much different frequency.

3. Flight tests were conducted to measure subcritical response of the horizontal tail to random inputs. The Peak-Hold and Randomdec methods were used to analyze the response data and to predict the onset of flutter for two response peaks. One peak at 45 to 46 Hz correlated well with theoretical predictions up to the maximum flight speed of 220 mph. The other peak at 27 to 28 Hz, however, did not correlate with theory. Although the origin of this response is not believed to be flutter related, the subcritical-response methods were used to predict an instability onset at 237 mph. Two possible causes for this response include forced vibration of the tail excited by a vibrating landing-gear door and extraneous electrical signals in the data. No flutter was observed during the flight tests.

4. The airplane was placarded at 205 mph to provide a safety margin during flights to study natural laminar flow over wing surfaces. This placard should remain in effect until further investigation is made to determine the origin of the response of 27 to 28 Hz observed on the horizontal tail.

Langley Research Center
National Aeronautics and Space Administration
Hampton, VA 23665
August 26, 1982

REFERENCES

1. Holmes, B. J.; and Obara, C. J.: Observations and Implications of Natural Laminar Flow on Practical Airplane Surfaces. ICAS Paper No. 82-5.1.1, Aug. 1982.

2. Gauzy, H.: Measurement of Inertia and Structural Damping. AGARD Manual on Aeroelasticity, Part IV, Chapter 3, Oct. 1968.

3. Redman, M. C.; and Rowe, W. S.: Prediction of Unsteady Aerodynamic Loadings Caused by Leading Edge and Trailing Edge Control Surface Motions in Subsonic Compressible Flow - Computer Program Description. NASA CR-132634, 1975.

4. Desmarais, Robert N.; and Bennett, Robert M.: User's Guide for a Modular Flutter Analysis Software System (FAST Version 1.0). NASA TM-78720, 1978.

5. Ruhlin, Charles L.; Watson, Judith J.; Ricketts, Rodney H.; and Doggett, Robert V., Jr.: Evaluation of Four Subcritical Response Methods for On-Line Prediction of Flutter Onset in Wind-Tunnel Tests. A Collection of Technical Papers, Part 2: Structural Dynamics and Design Engineering - AIAA/ASME/ASCE/AHS 23rd Structures, Structural Dynamics and Materials Conference, May 1982, pp. 94-101. (Available as AIAA-82-0644.)

6. Flutter Testing Techniques. NASA SP-415, 1976.

7. Regier, A. A.: Flutter of Control Surfaces and Tabs. Manual on Aeroelasticity, Volume V, AGARD, Feb. 1960, Part V, Chapter 3.

TABLE I.- GRID POINTS FOR MEASURING GROUND-VIBRATION TEST MODELS

Grid point	x, in.	y, in.	Grid point	x, in.	y, in.
1	38.94	81.98	21	41.13	40.99
2	31.92		22	31.92	
3	29.11		23	28.23	
4	23.21		24	20.50	
5	16.75		25	12.02	
6	39.49	71.74	26	41.68	30.74
7	31.92		27	31.92	
8	28.89		28	28.02	
9	22.53		29	19.82	
10	15.57		30	10.84	
11	40.04	61.49	31	42.23	20.50
12	31.92		32	31.92	
13	28.67		33	27.80	
14	21.85		34	19.14	
15	14.39		35	9.66	
16	40.59	51.24	36	42.77	10.25
17	31.92		37	31.92	
18	28.45		38	27.58	
19	21.18		39	18.46	
20	13.20		40	8.48	
			41	43.32	0
			42	31.92	0

TABLE II.- GROUND-VIBRATION TEST RESULTS FOR SYMMETRIC MODES

(a) Frequency, generalized mass, and structural damping

	Mode number (type)				
	1 (stabilizer)	2 (elevator)	3 (elevator)	4 (stabilizer)	5 (stabilizer)
f, Hz	8.77	19.5	22.0	39.2	49.8
m_g, slugs	1.1 to 1.6	1.5 to 1.6	1.4 to 1.7	27 to 38	5.5 to 29
g	0.019	0.049	0.046	0.031	0.02 to 0.06
*f_{1975}, Hz	10.2	12.8	12.8	39.0	54.0
**Δf, percent	-14	52	72	1	-8

*f_{1975} denotes frequencies measured by manufacturer in 1975.

**Δf is calculated as $\left(1 - \frac{f}{f_{1975}}\right) \times 100$.

TABLE II.- Continued

(b) Displacements normalized on grid point 1

Grid point	Vertical displacement of the ith mode, z(i)				
	z(1)	z(2)	z(3)	z(4)	z(5)
1	1.000	1.000	1.000	1.000	1.000
2	1.008	.059	.176	2.830	-.158
3	.980	-.146	.189	-4.113	-.297
4	.953	0	.126	-3.094	2.424
5	.949	0	.071	-5.622	3.939
6	0.745	1.494	1.220	-1.585	-1.242
7	.792	.264	.244	-2.076	-2.757
8	.757	0	.181	-1.660	-.539
9	.745	0	.105	-3.622	1.000
10	.710	0	.063	-6.113	2.576
11	0.498	1.647	1.315	-1.528	-2.576
12	.537	.376	.307	-2.641	-4.606
13	.533	0	.118	-2.132	-1.515
14	.514	0	.083	-4.000	.303
15	.471	0	.061	-6.113	1.424
16	0.294	1.812	1.315	-0.679	-2.121
17	.341	.471	.189	-2.151	-4.758
18	.325	0	.068	-2.038	-2.106
19	.306	0	.068	-3.642	-.864
20	.286	0	.088	-5.132	.621

TABLE II.- Concluded

(b) Concluded

Grid point	Vertical displacement of the ith mode, z(i)				
	z(1)	z(2)	z(3)	z(4)	z(5)
21	0.129	1.812	1.244	2.415	-0.461
22	.180	.412	.106	-.943	-3.394
23	.176	0	.063	-1.396	-2.333
24	.169	0	.069	-2.717	-1.091
25	.122	0	.121	-4.075	.297
26	0.020	1.976	1.244	4.377	1.939
27	.051	.400	.065	.698	-2.182
28	.037	0	.076	-.200	-1.848
29	.029	0	.099	-1.604	-.969
30	.016	0	-.145	-2.755	.242
31	-0.069	1.847	1.236	5.660	3.212
32	-.043	.318	.091	1.358	-1.242
33	-.059	0	.131	.736	-1.167
34	-.065	0	-.142	-.604	-.588
35	-.078	0	-.181	-1.528	.182
36	-0.118	1.882	1.228	6.491	4.545
37	-.098	.282	.126	1.509	-.524
38	-.110	0	0	1.132	-.445
39	-.114	0	-.168	.566	-.154
40	-.122	0	-.192	-.566	.282
41	-0.155	1.860	1.102	6.604	5.151
42	-.124	.210	.150	1.550	-.200

TABLE III.- GROUND-VIBRATION TEST RESULTS FOR ANTISYMMETRIC MODES

(a) Frequency and generalized mass

	Mode number (type)		
	1 (stabilizer)	2 (elevator)	3 (elevator)
f, Hz	6.06	27.2	43.4
m_q, slugs	1.1 to 1.4	4.7 to 6.0	0.5 to 0.7
*f_{1975}, Hz	8.4	25.5	46.0
**Δf, percent	-28	7	-6

*f_{1975} denotes frequencies measured by manufacturer in 1975.

**Δf is calculated as $\left(1 - \frac{f}{f_{1975}}\right) \times 100$.

TABLE III.- Continued

(b) Displacements normalized on grid point 1

Grid point	Vertical displacement of the ith mode, z(i)		
	z(1)	z(2)	z(3)
1	1.000	1.000	1.000
2	.970	-.853	.383
3	.956	-1.600	.214
4	1.038	-.337	-.107
5	1.010	-.195	-.423
6	0.874	2.474	1.232
7	.820	.937	.554
8	.831	.389	.049
9	.820	.432	-.264
10	.798	.442	-.597
11	0.661	2.842	1.217
12	.683	1.789	.496
13	.667	.842	-.130
14	.634	.905	-.380
15	.601	.895	-.623
16	0.530	3.368	0.942
17	.508	1.853	.270
18	.508	1.137	-.209
19	.486	1.105	-.441
20	.470	1.084	-.638

TABLE III.- Concluded

(b) Concluded

Grid point	Vertical displacement of the ith mode, z(i)		
	z(1)	z(2)	z(3)
21	0.372	2.632	0.522
22	.399	1.421	.014
23	0.372	1.316	-.188
24	.361	1.211	-.380
25	.350	1.158	-.565
26	0.268	2.000	0.243
27	.273	1.158	-.125
28	.260	1.116	-.159
29	.251	1.032	-.275
30	.230	.958	-.443
31	0.158	1.379	0.130
32	.169	.832	-.148
33	.153	.684	-.130
34	.142	.653	-.186
35	.123	.526	-.275
36	0.068	0.768	-0.090
37	.077	.305	-.101
38	.071	.311	-.072
39	.055	.263	-.081
40	.044	.184	-.128
41	0.015	0.084	0.042
42	.016	.032	.028

TABLE IV.- EIGENVECTORS FOR FLUTTER MODES FROM ANALYSIS AT M = 0.3

(a) Symmetric flutter mode; f = 45 Hz

Mode	Magnitude	Phase, deg
1	0.11	-25
2	.33	53
3	.24	48
4	.17	-82
5	1.00	0

(b) Antisymmetric flutter mode; f = 37 Hz

Mode	Magnitude	Phase, deg
1	0.20	43
2	.13	59
3	1.00	0

L-82-3003

Figure 1.- Photograph of Skyrocket II airplane.

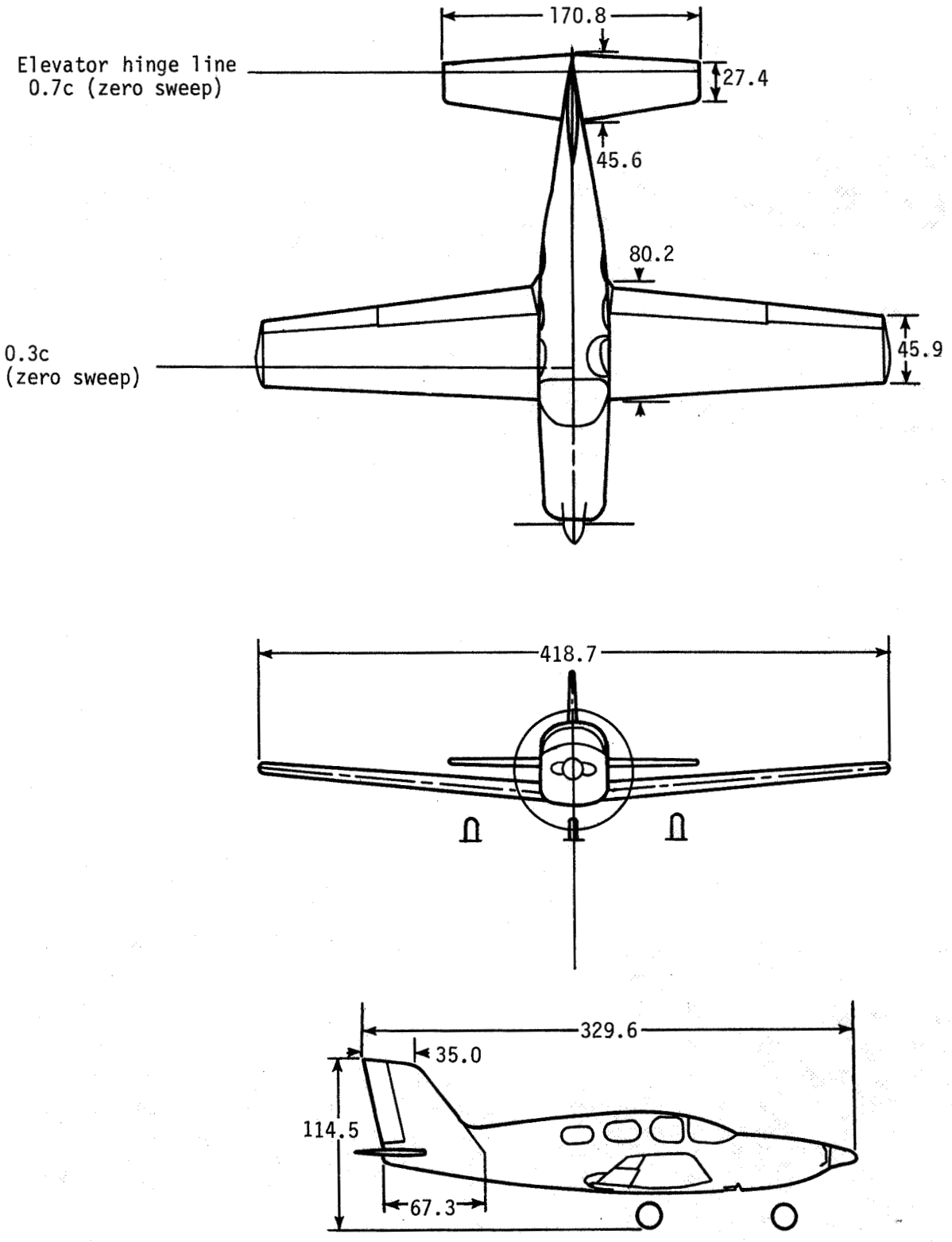

Figure 2.- A three-view drawing of Skyrocket II airplane. Dimensions are given in inches.

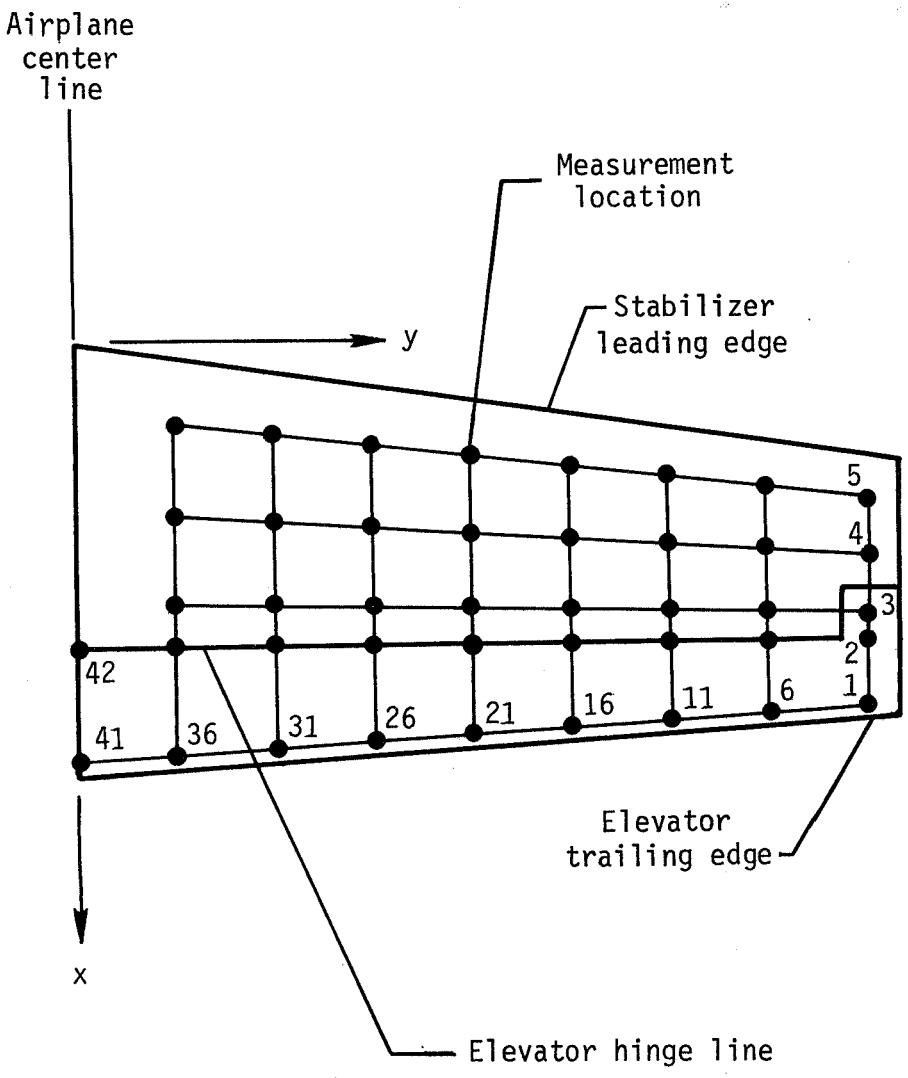

Figure 3.- Measurement locations for horizontal-tail GVT.

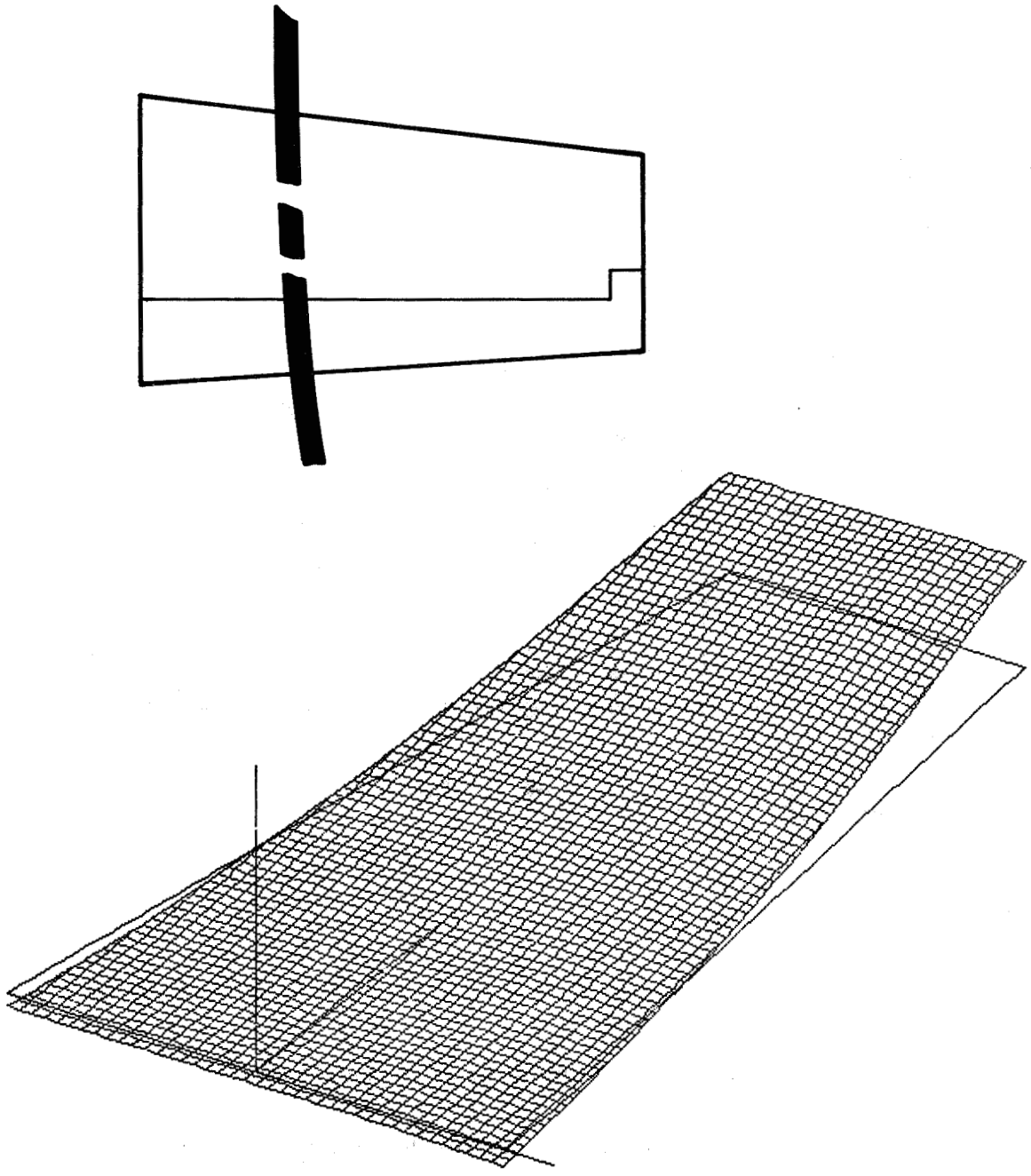

(a) Mode 1; stabilizer bending, 8.77 Hz.

Figure 4.- Symmetric GVT mode shapes.

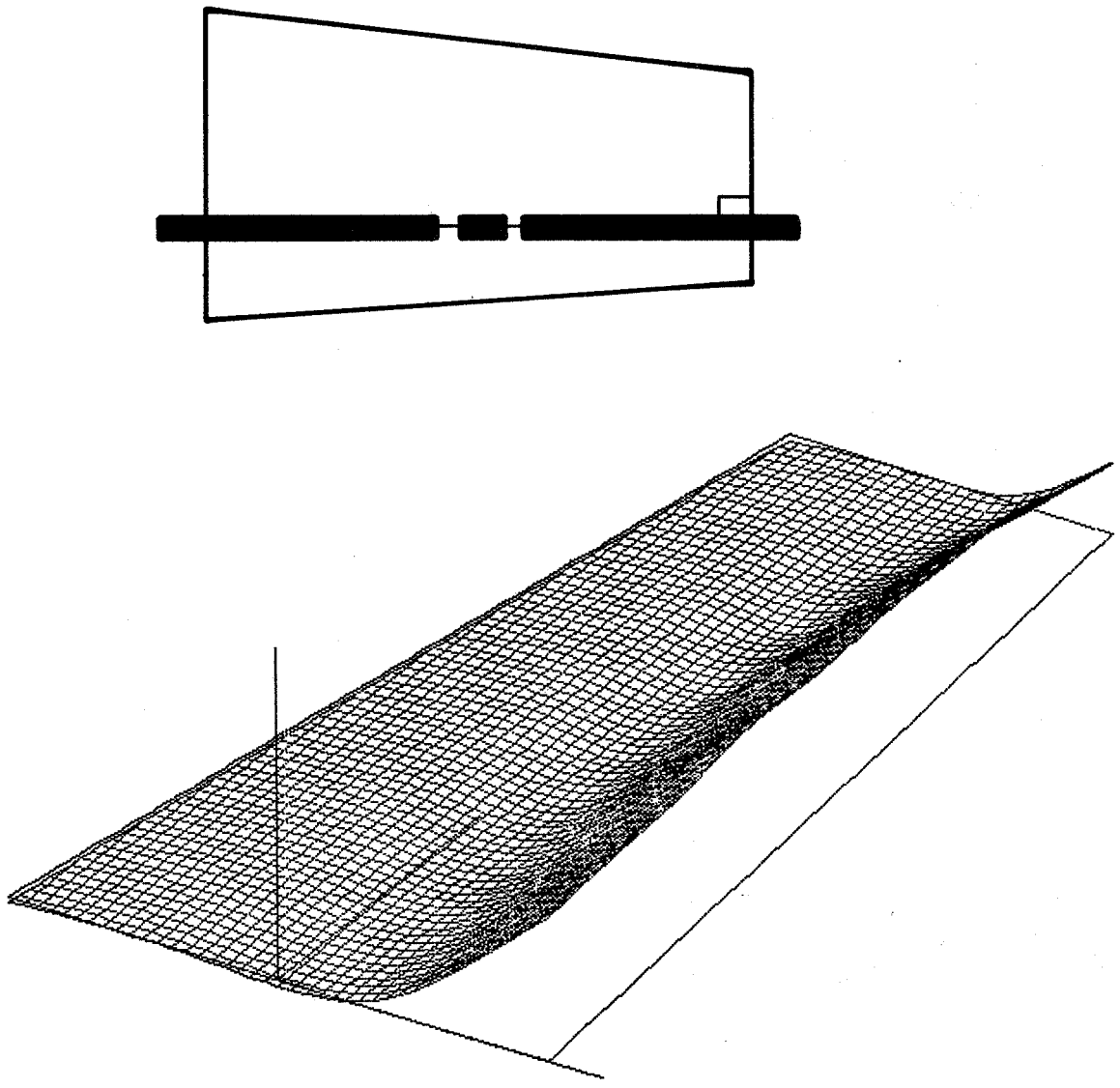

(b) Mode 2; elevator rotation, 19.5 Hz.

Figure 4.- Continued.

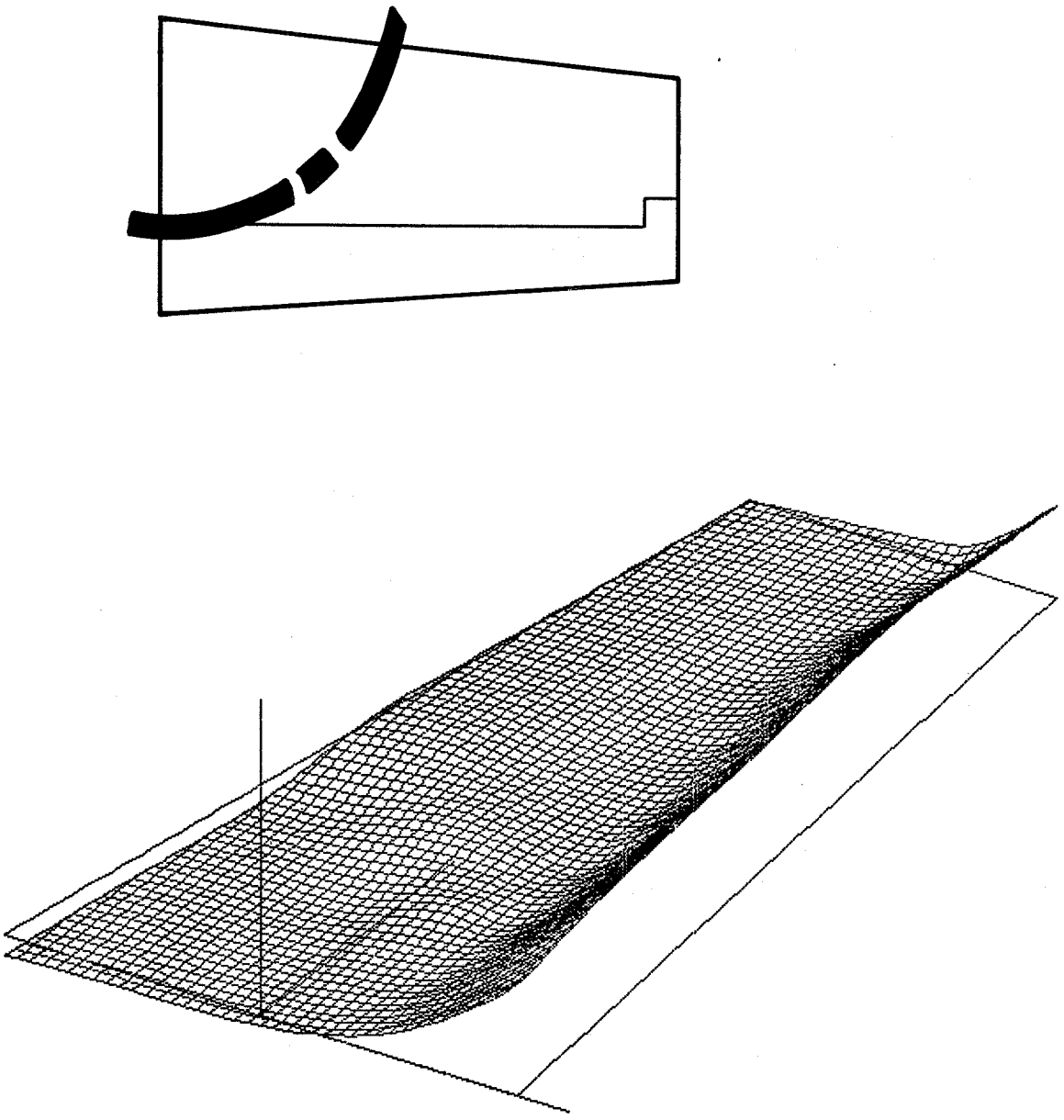

(c) Mode 3; elevator rotation, 22.0 Hz.

Figure 4.- Continued.

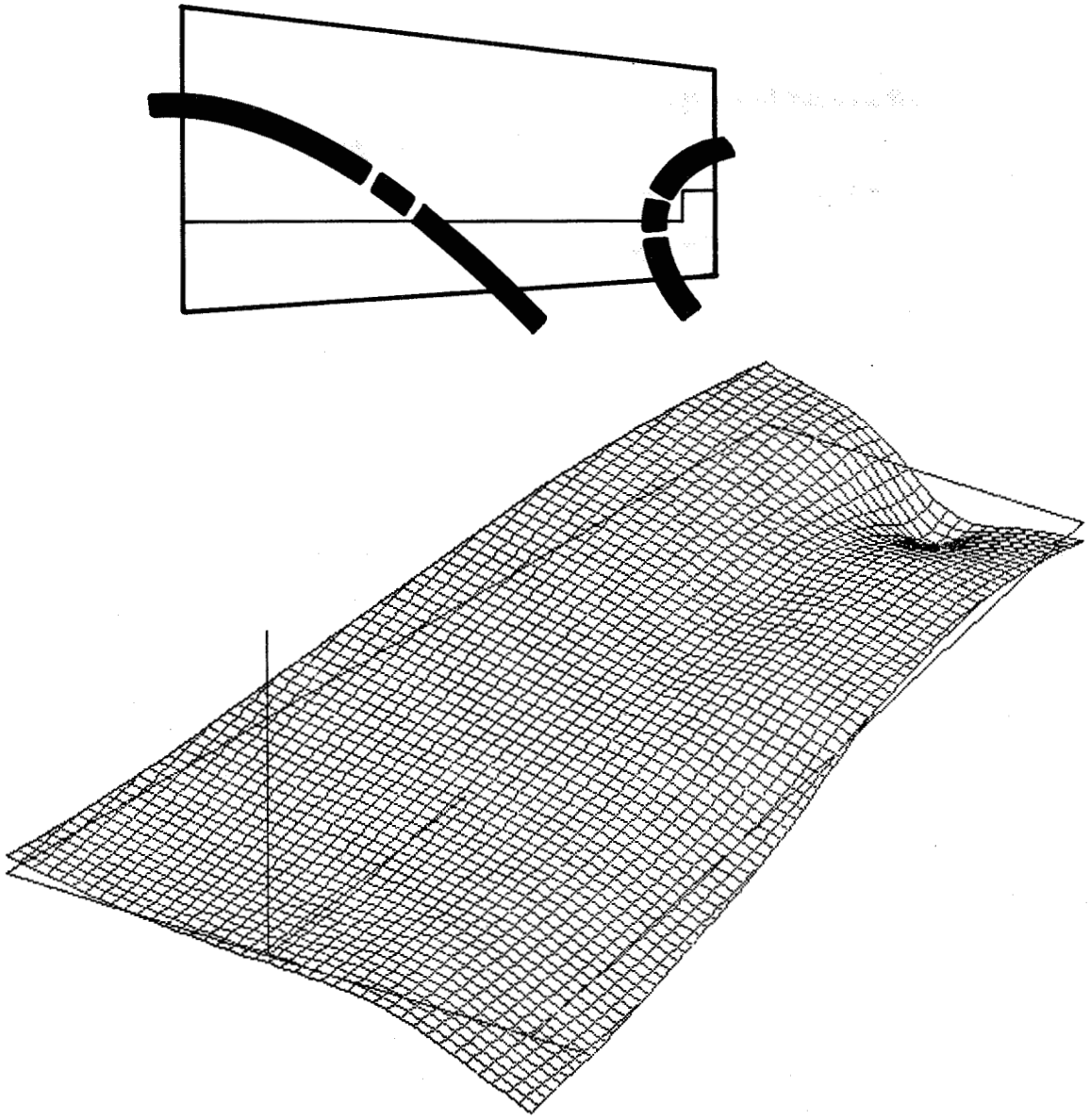

(d) Mode 4; stabilizer bending, 39.2 Hz.

Figure 4.- Continued.

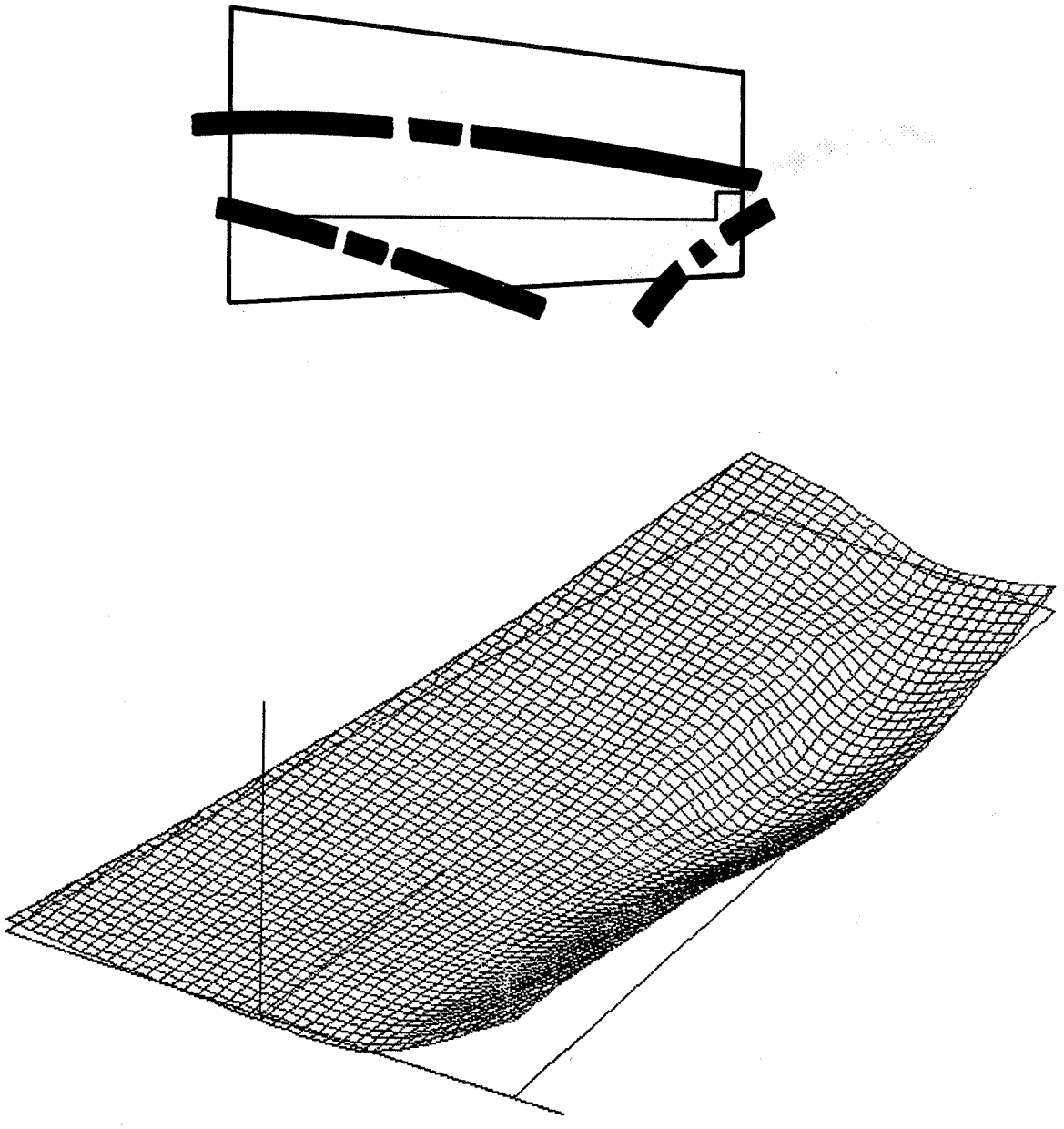

(e) Mode 5; stabilizer torsion, 49.8 Hz.

Figure 4.- Concluded.

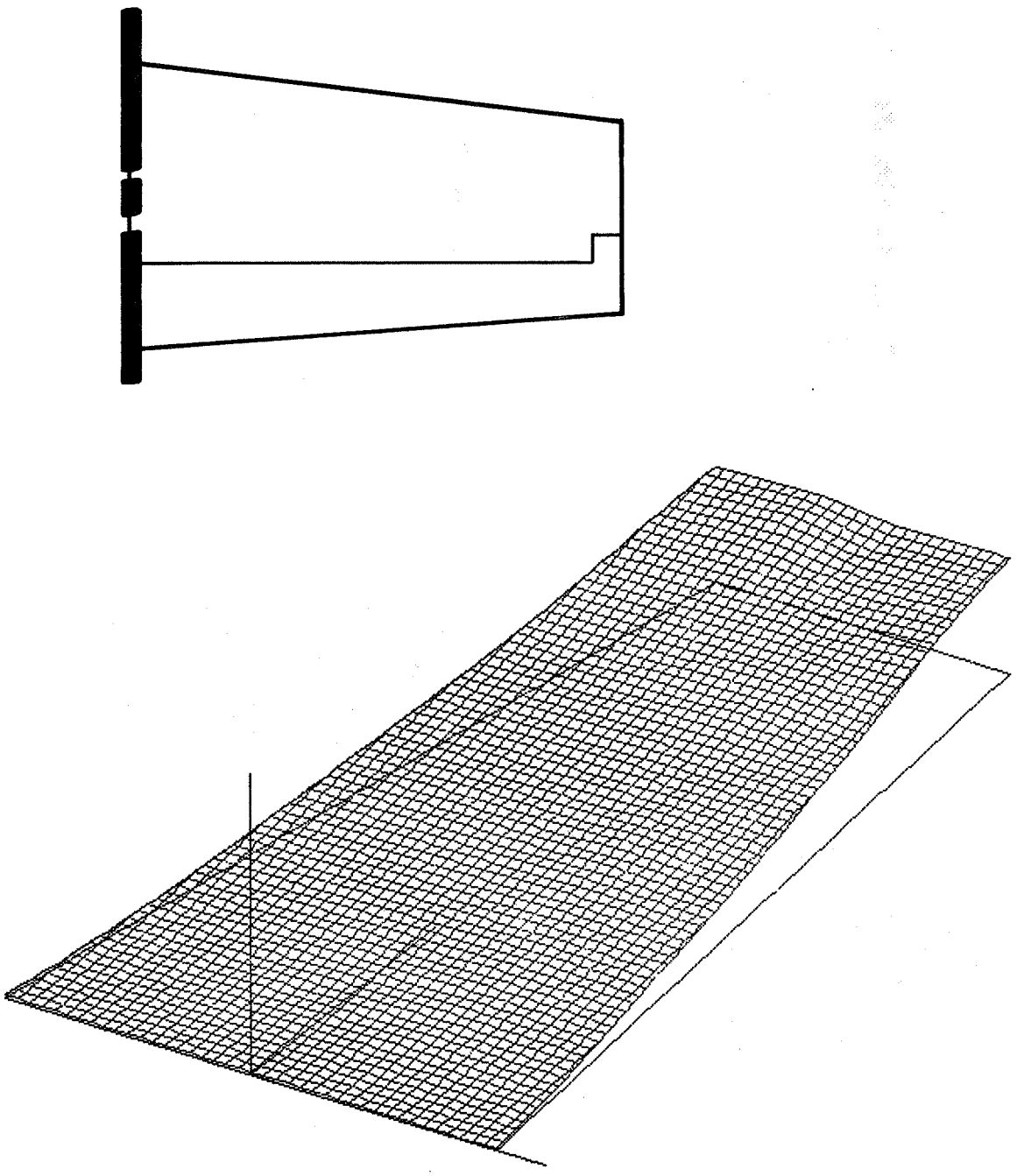

(a) Mode 1; stabilizer bending, 6.06 Hz.

Figure 5.- Antisymmetric GVT mode shapes.

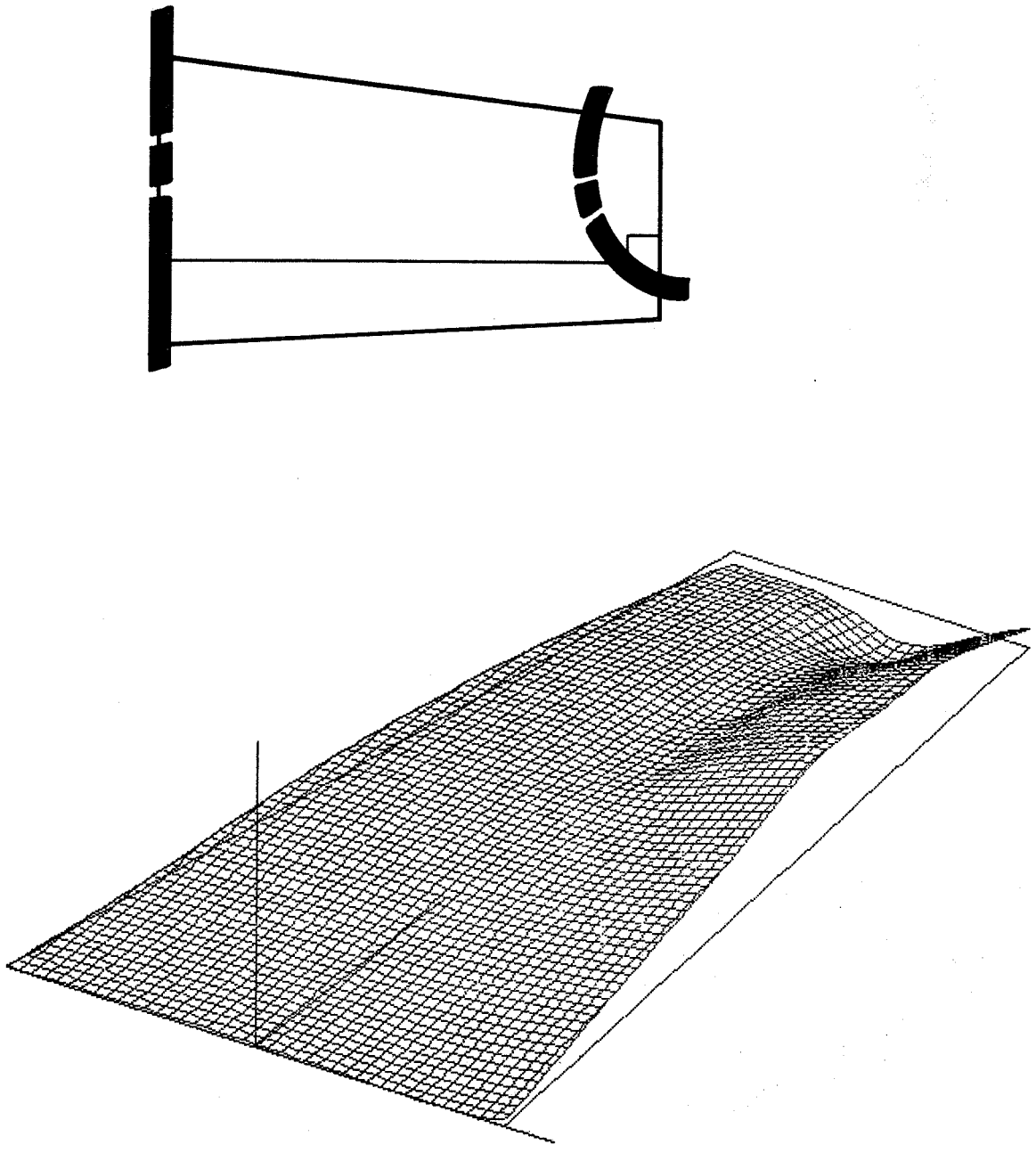

(b) Mode 2; elevator bending, 27.2 Hz.

Figure 5.- Continued.

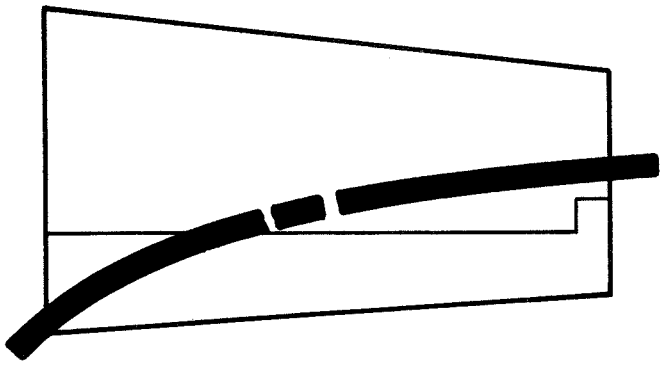

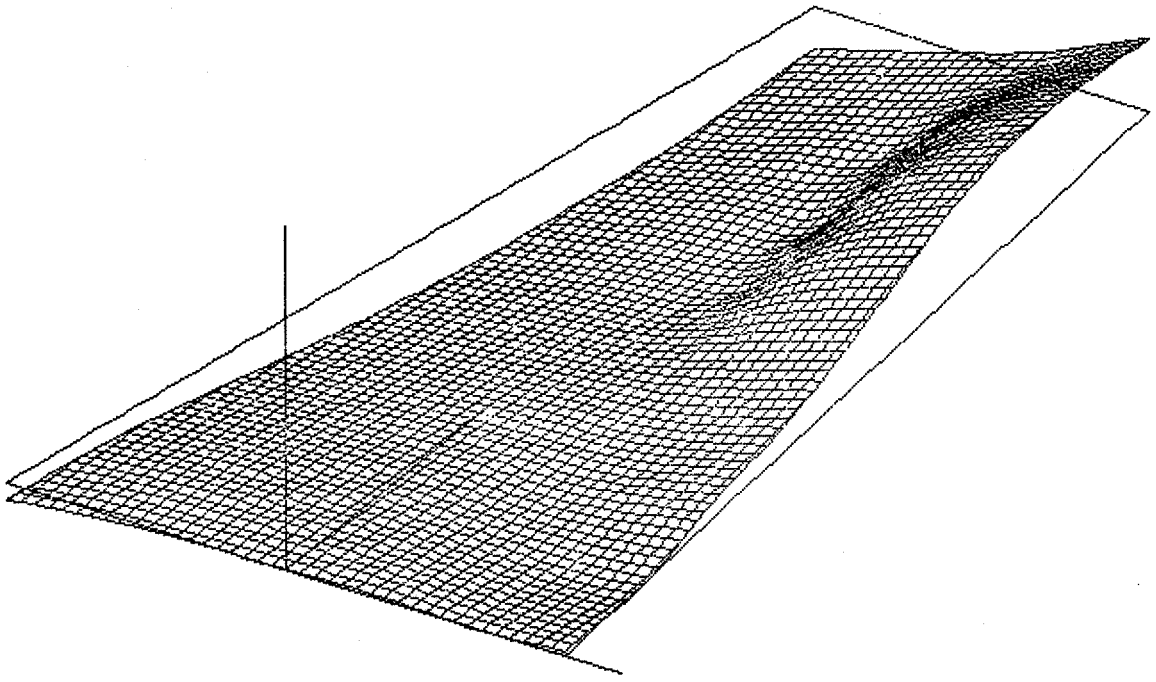

(c) Mode 3; elevator torsion, 43.4 Hz.

Figure 5.- Concluded.

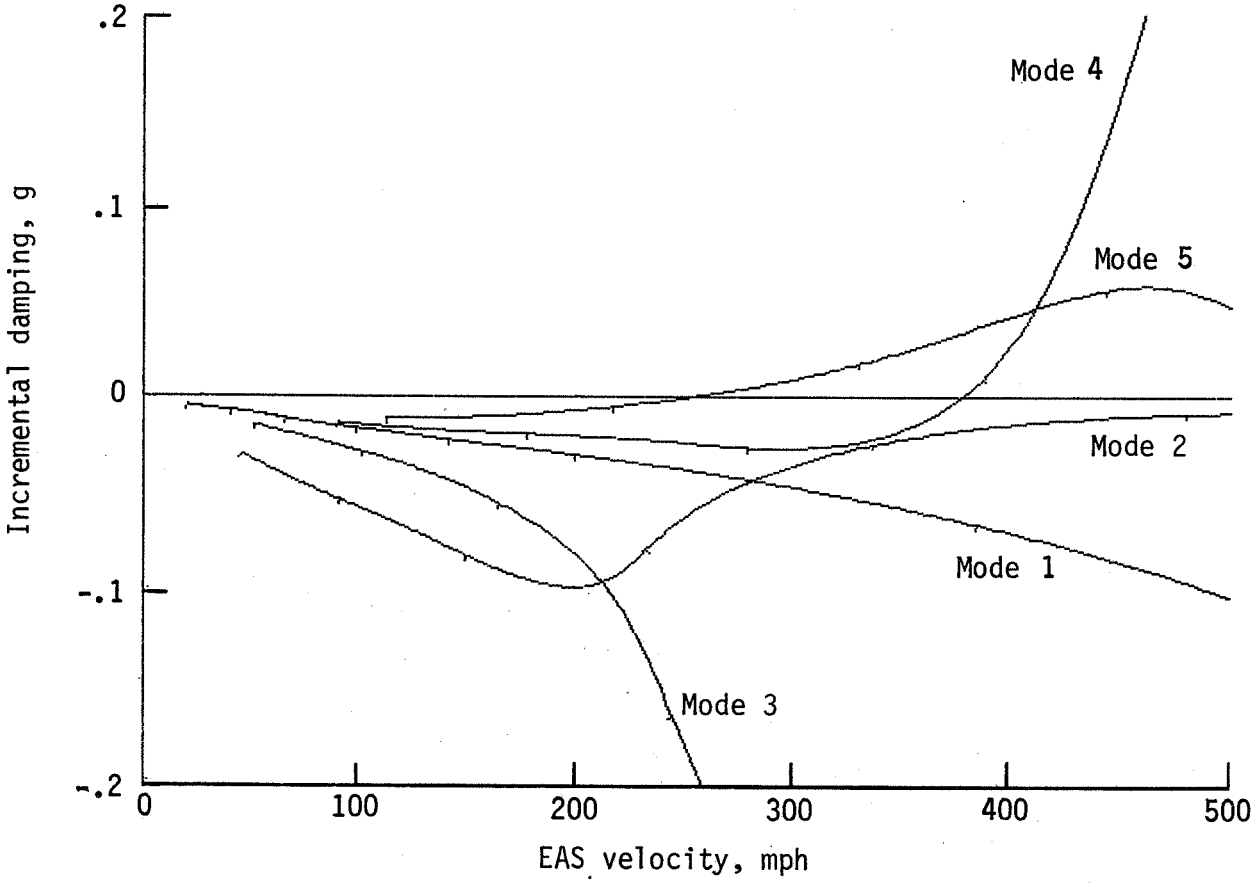

(a) Velocity-damping (V-g) plot.

Figure 6.- Typical results of symmetric-flutter analysis. h = 10 000 ft; M = 0.3.

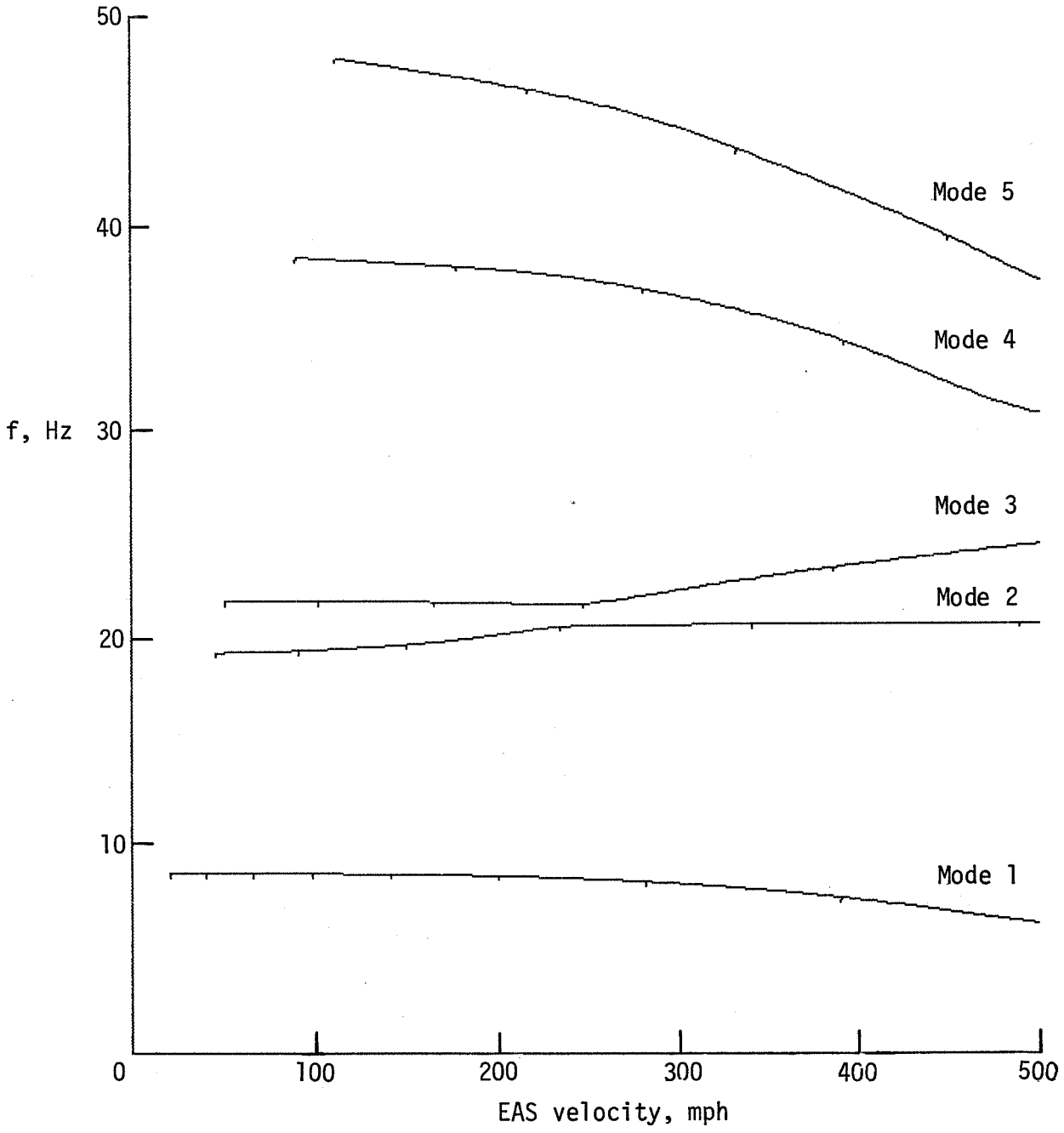

(b) Velocity-frequency (V-f) plot.

Figure 6.- Concluded.

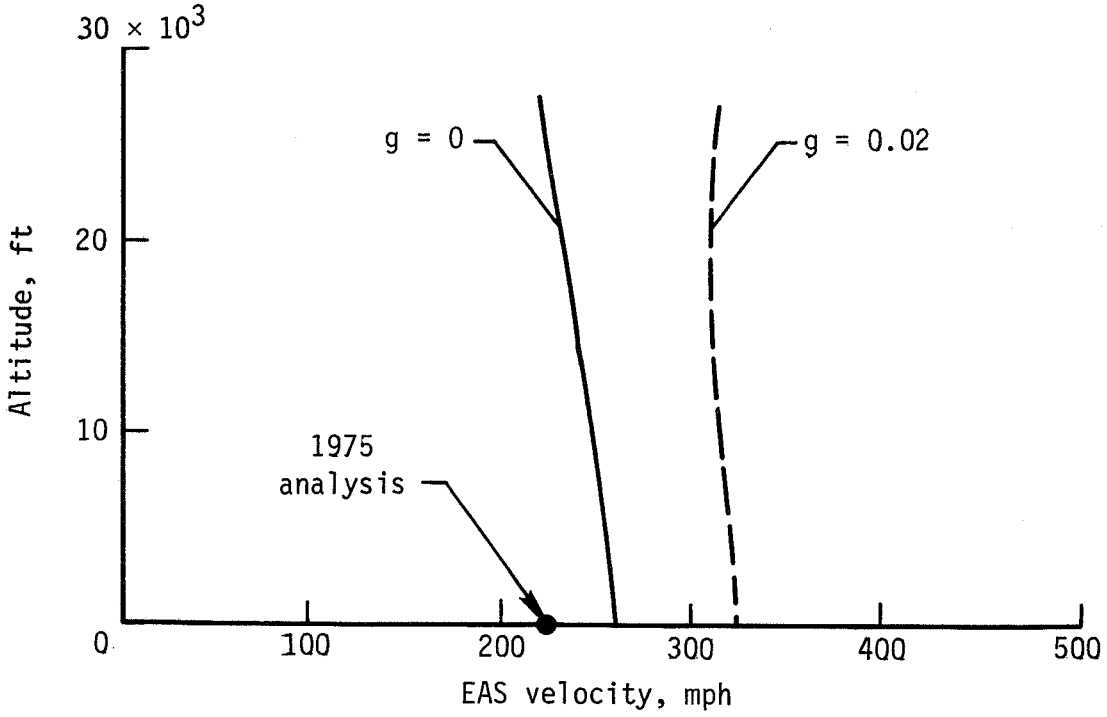

Figure 7.- Symmetric flutter boundaries from analyses with two values of structural damping.

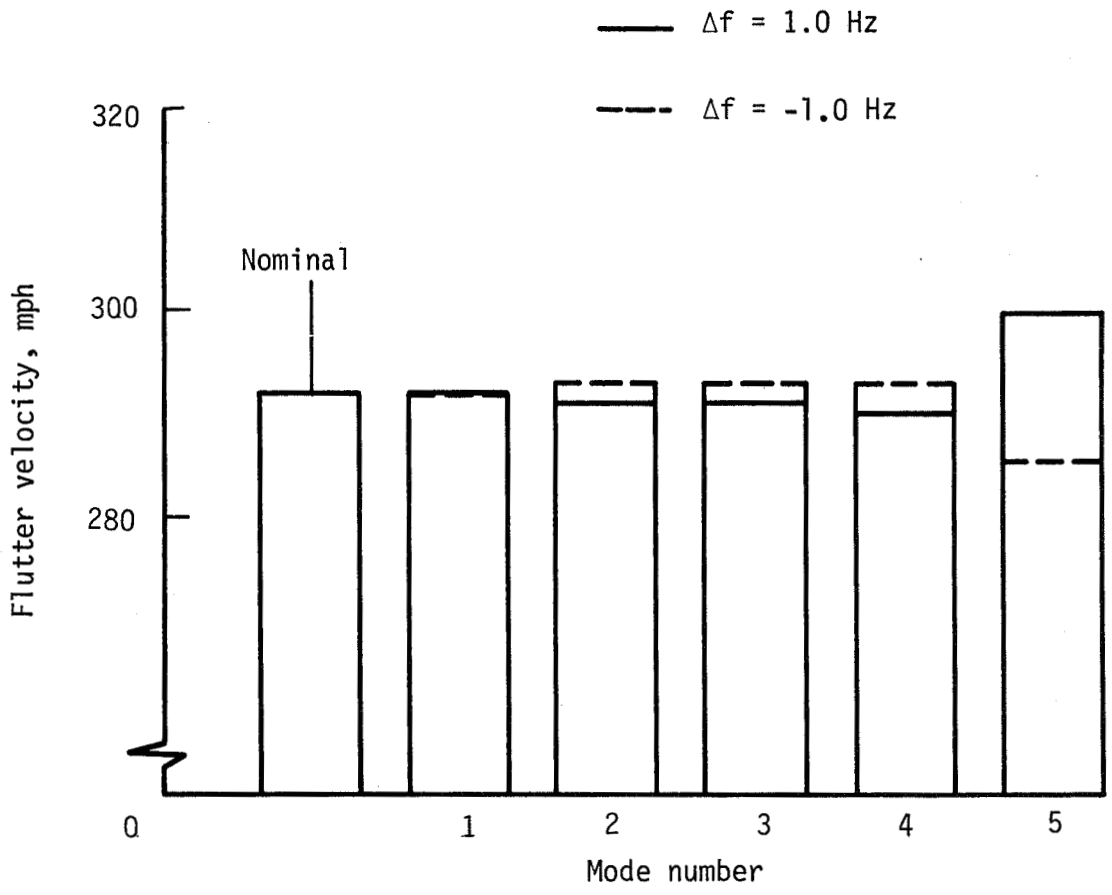

(a) Incremental changes in individual GVT modal frequencies.

Figure 8.- Flutter-velocity sensitivity analysis. h = 12 500 ft; M = 0.4.

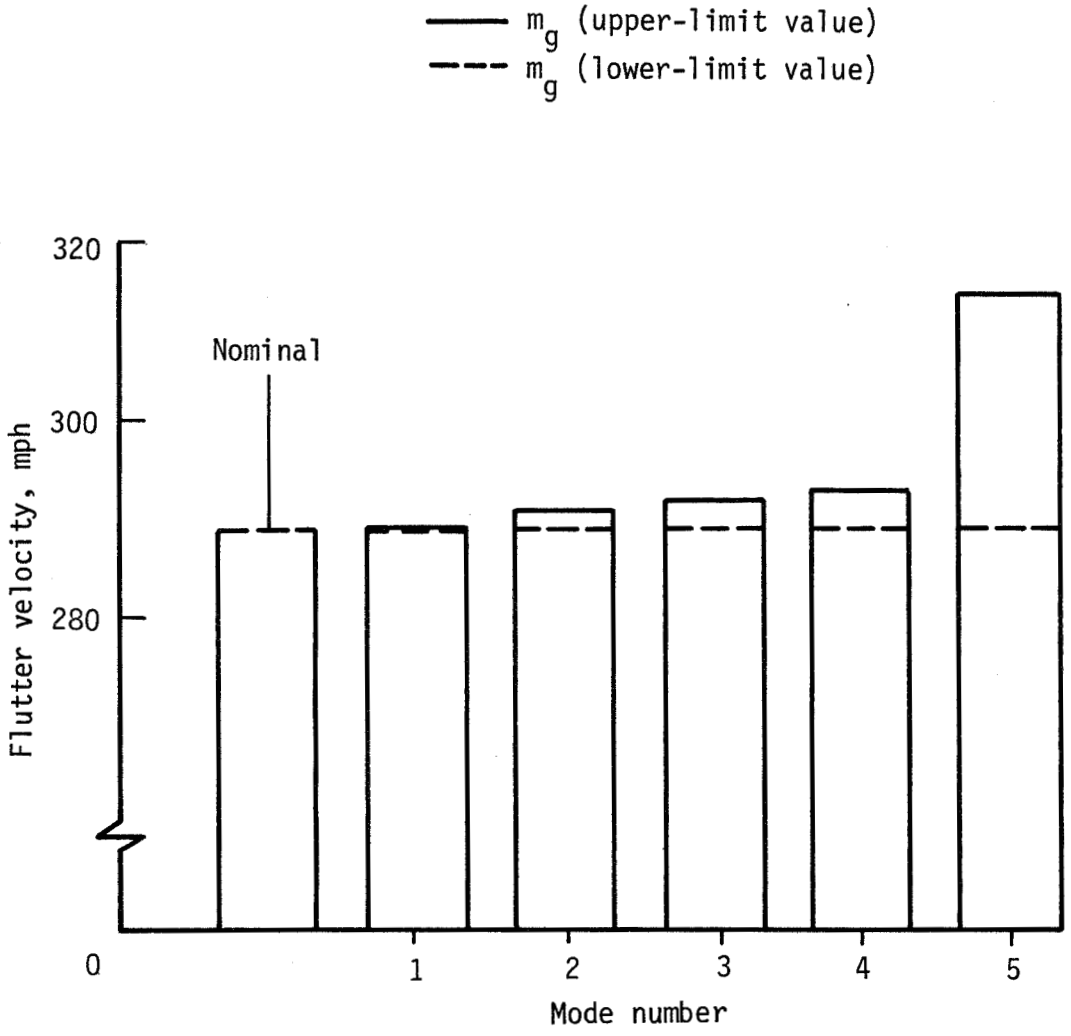

(b) Incremental changes in individual GVT modal generalized masses. (See table II for limit values.)

Figure 8.- Concluded.

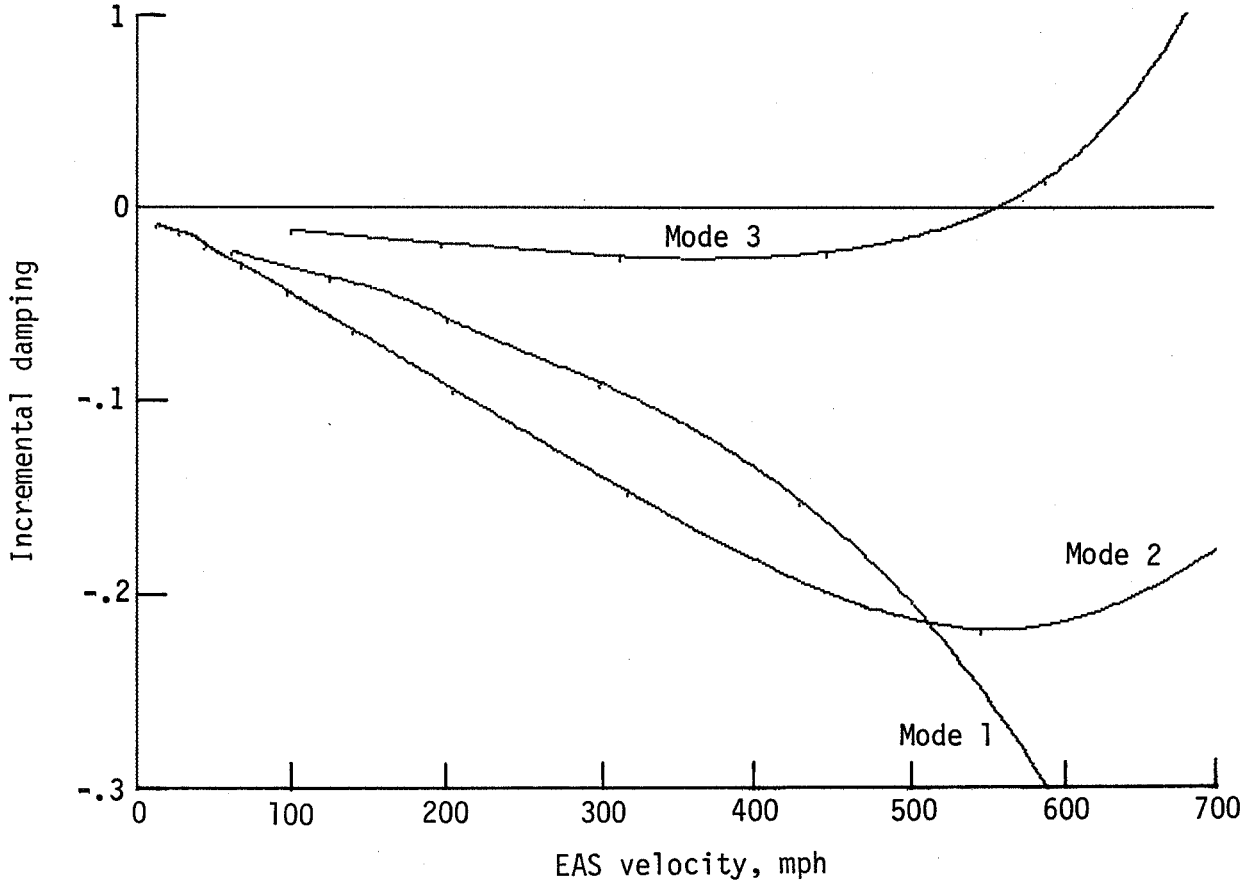

(a) Velocity-damping (V-g) plot.

Figure 9.- Typical results of antisymmetric-flutter analysis. h = 10 000 ft; M = 0.3.

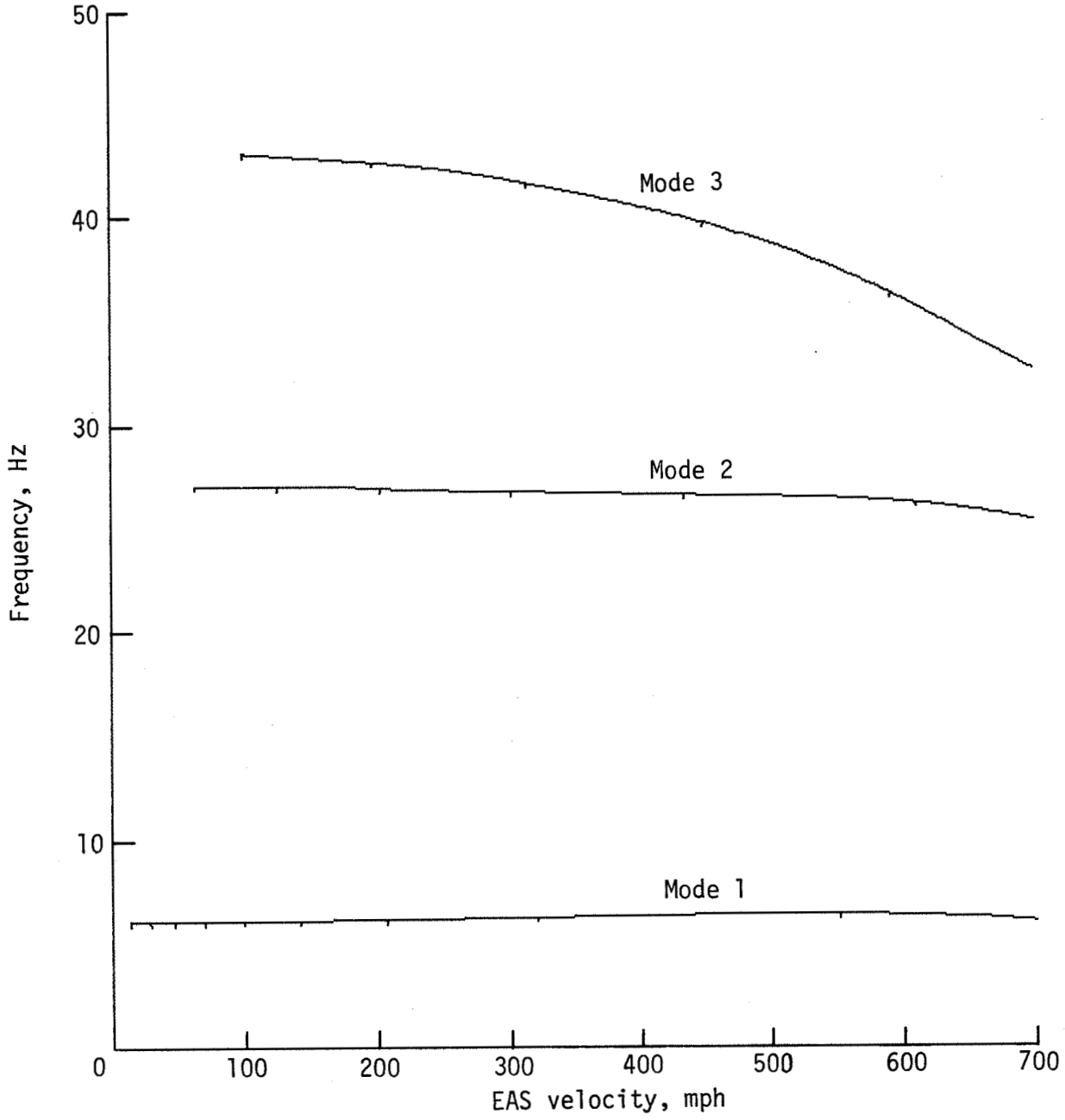

(b) Velocity-frequency (V-f) plot.

Figure 9.- Concluded.

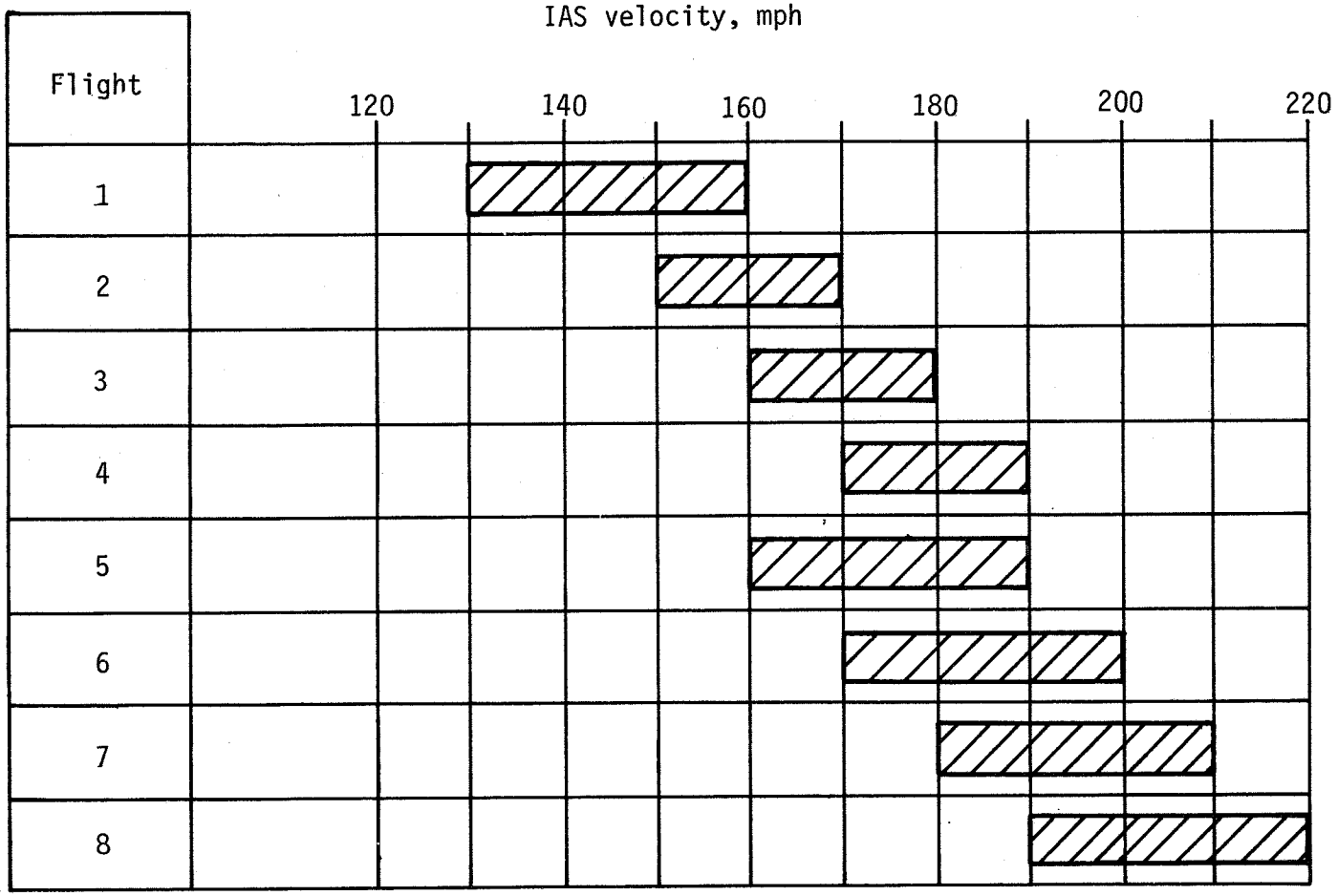

Figure 10.- Velocity ranges for flight data.

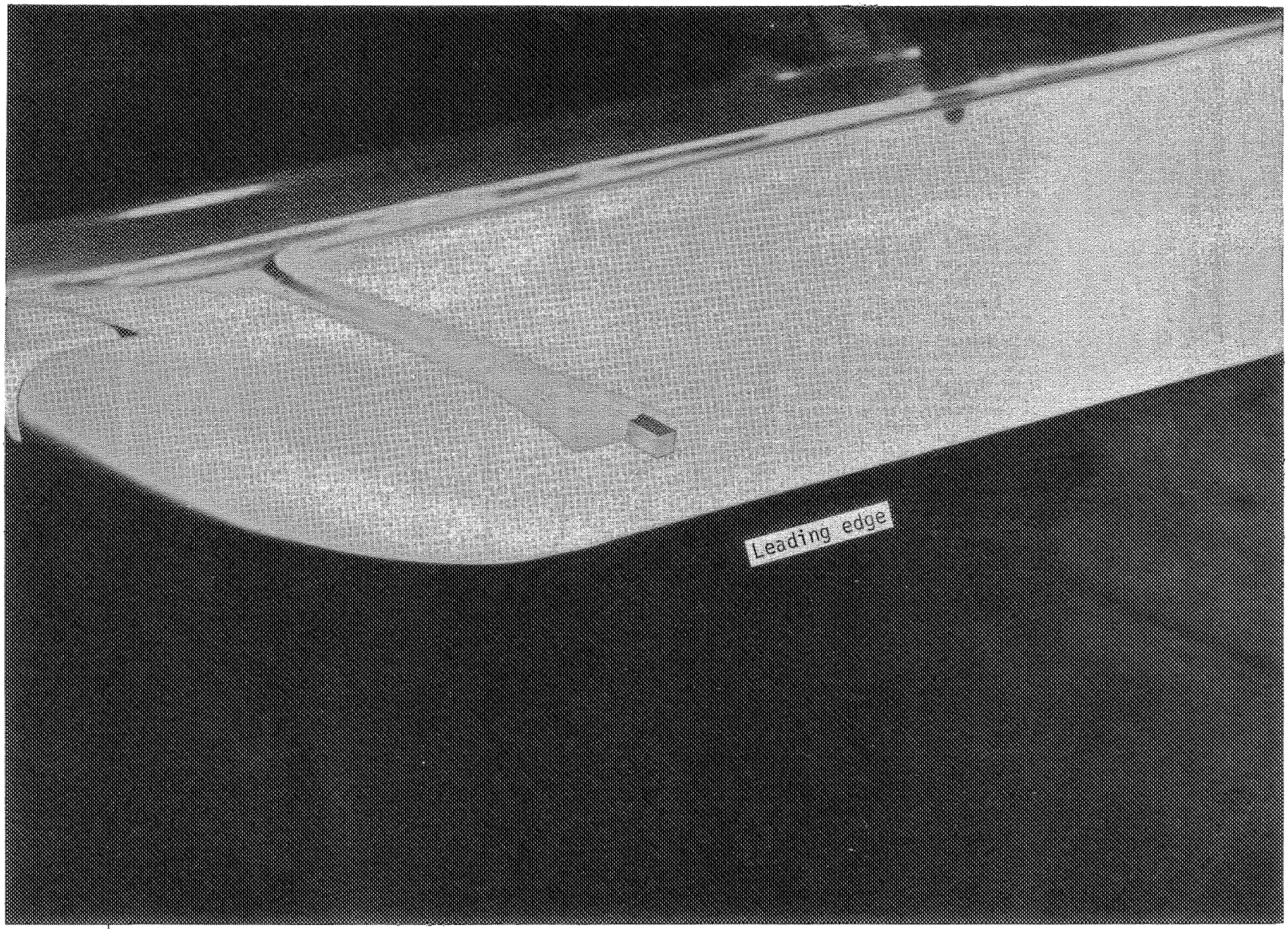

L-81-6424.1

(a) On stabilizer upper surface.

Figure 11.- Photograph of accelerometer installations.

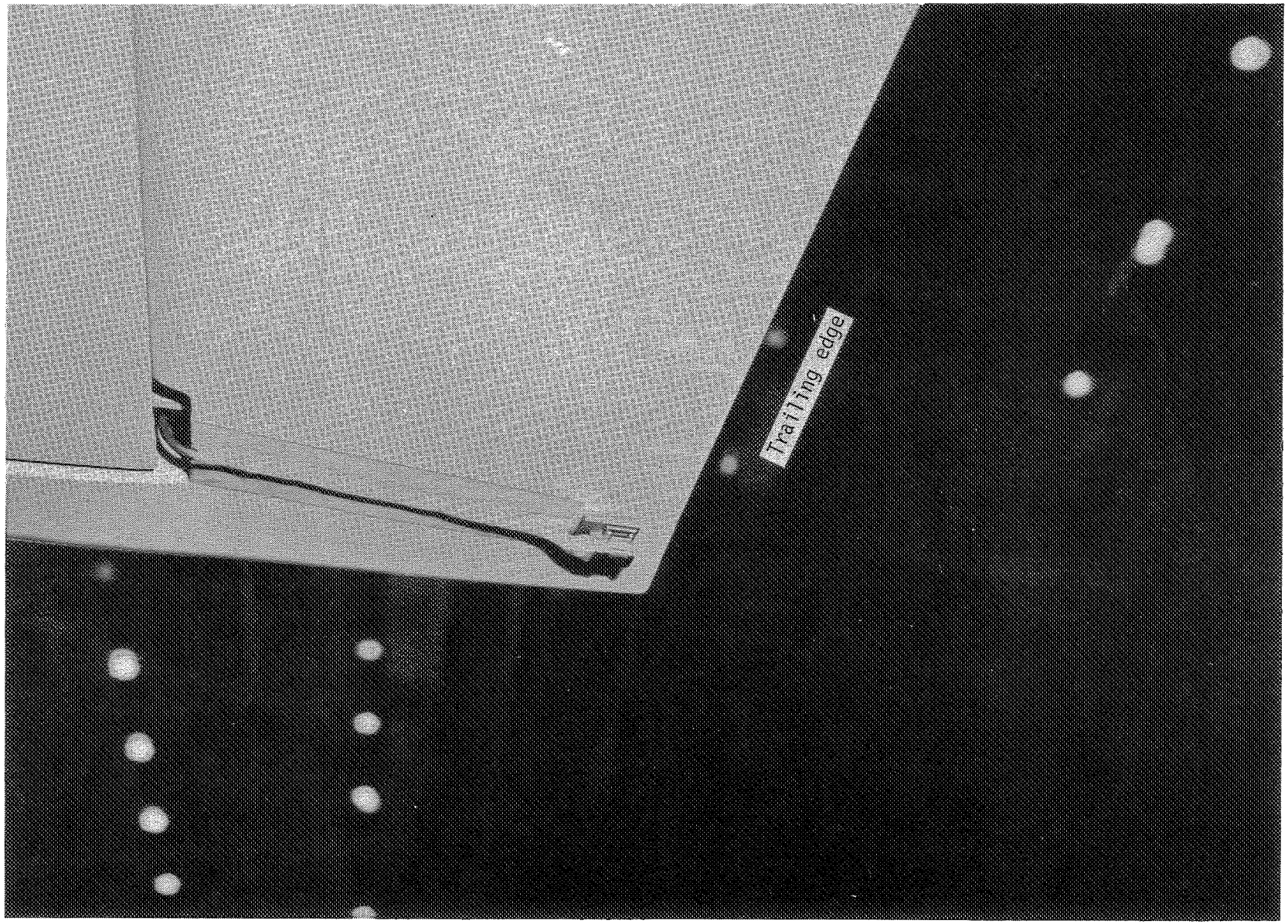

L-81-6425.1

(b) On elevator lower surface.

Figure 11.- Concluded.

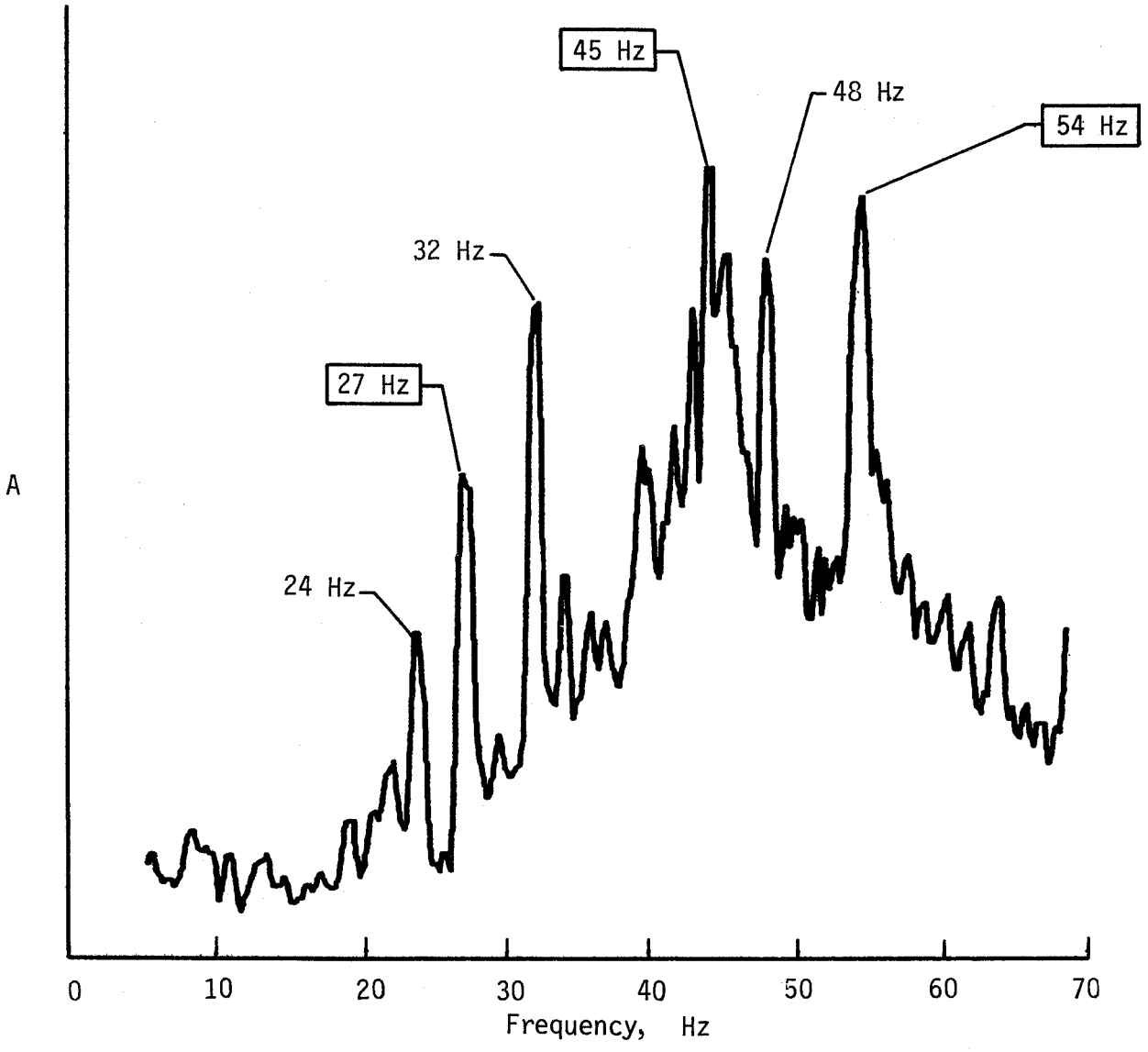

(a) Elevator.

Figure 12.- Peak-Hold frequency-response spectra for accelerometer data acquired at an IAS velocity of 220 mph.

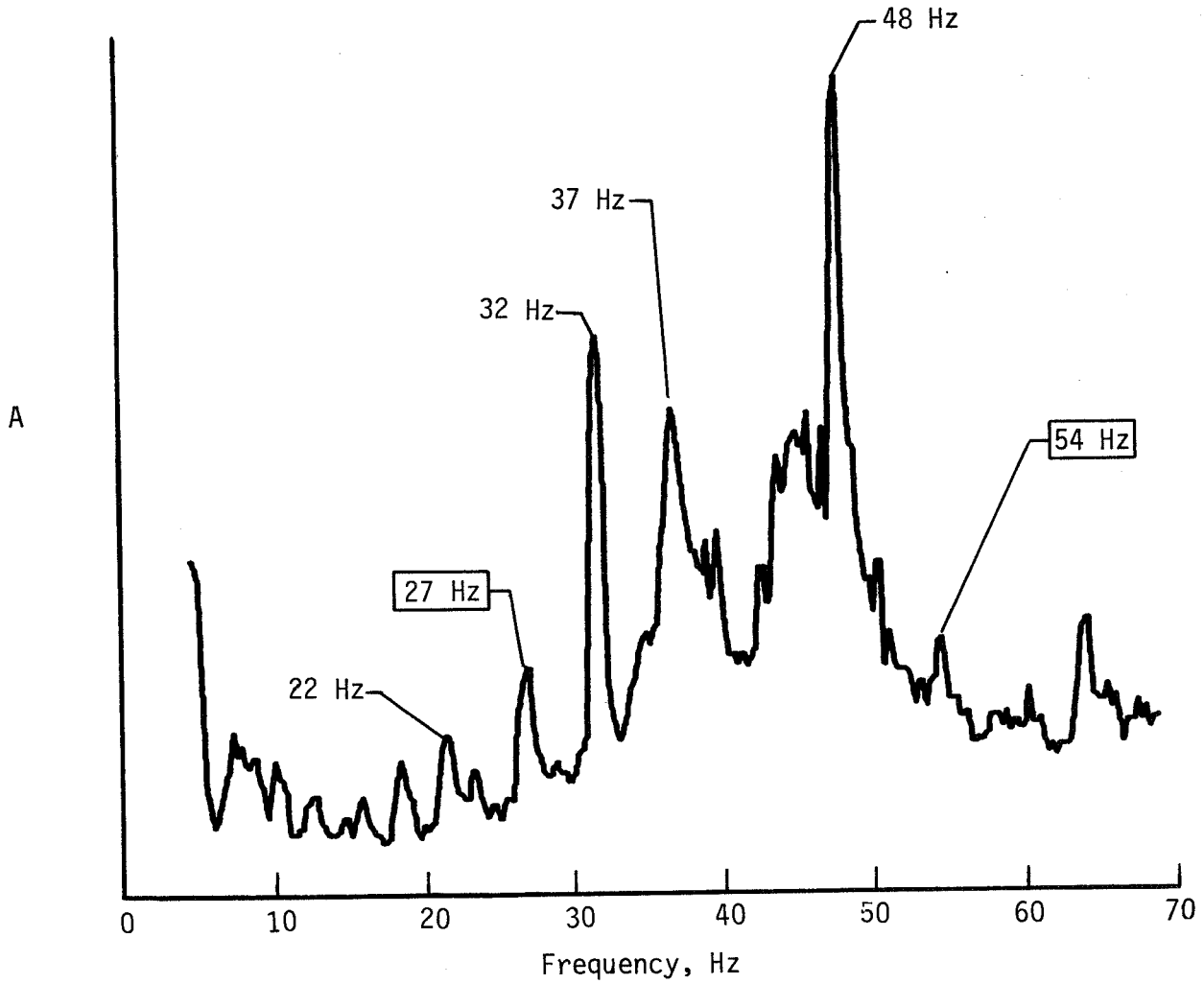

(b) Stabilizer.

Figure 12.- Concluded.

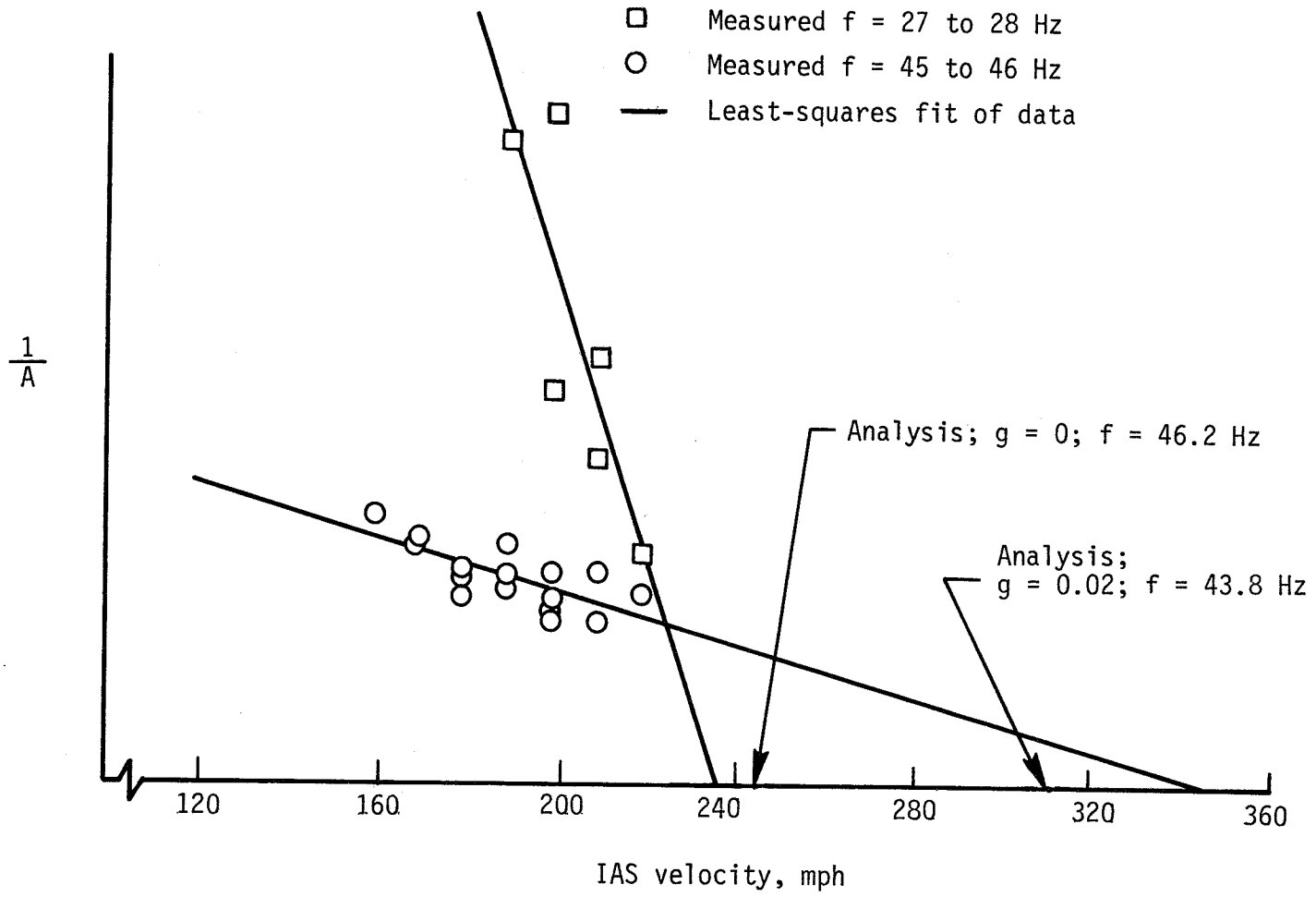

Figure 13.- Peak-Hold results for response at two frequencies for the elevator accelerometer at 10 000 ft.

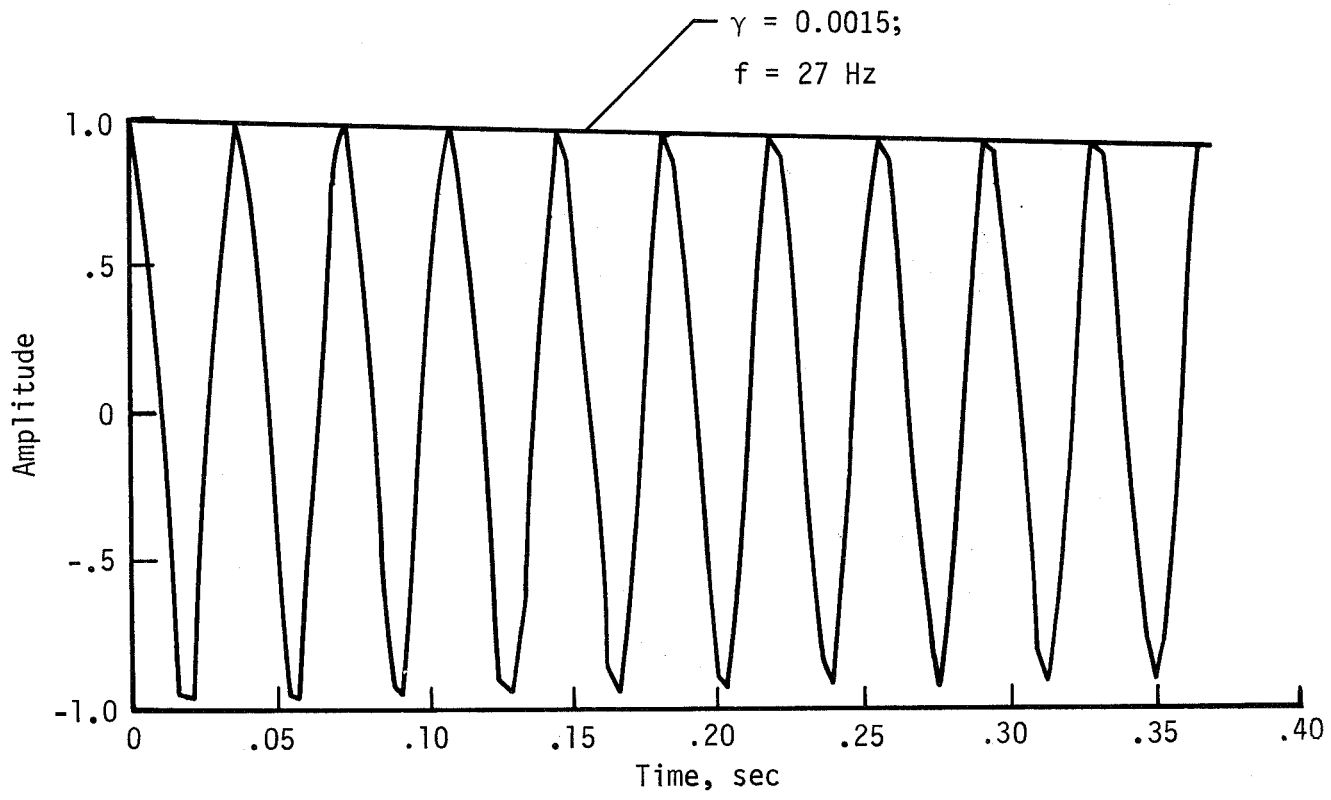

(a) 27-Hz mode.

Figure 14.- Randomdec signatures for response of elevator accelerometer at an IAS velocity of 220 mph.

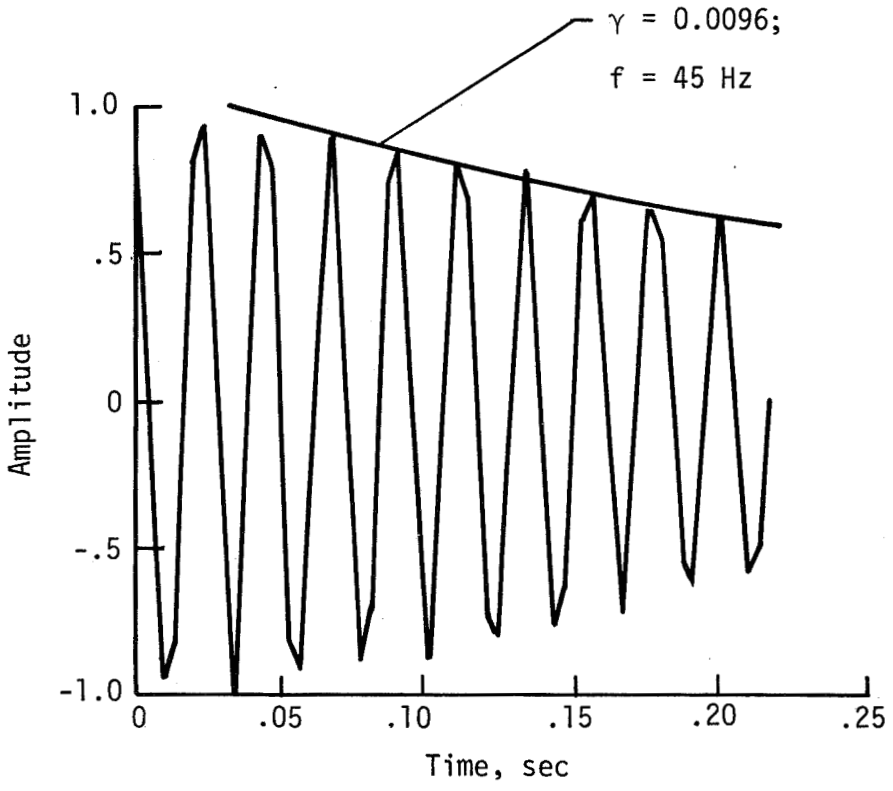

(b) 45-Hz mode.

Figure 14.- Concluded.

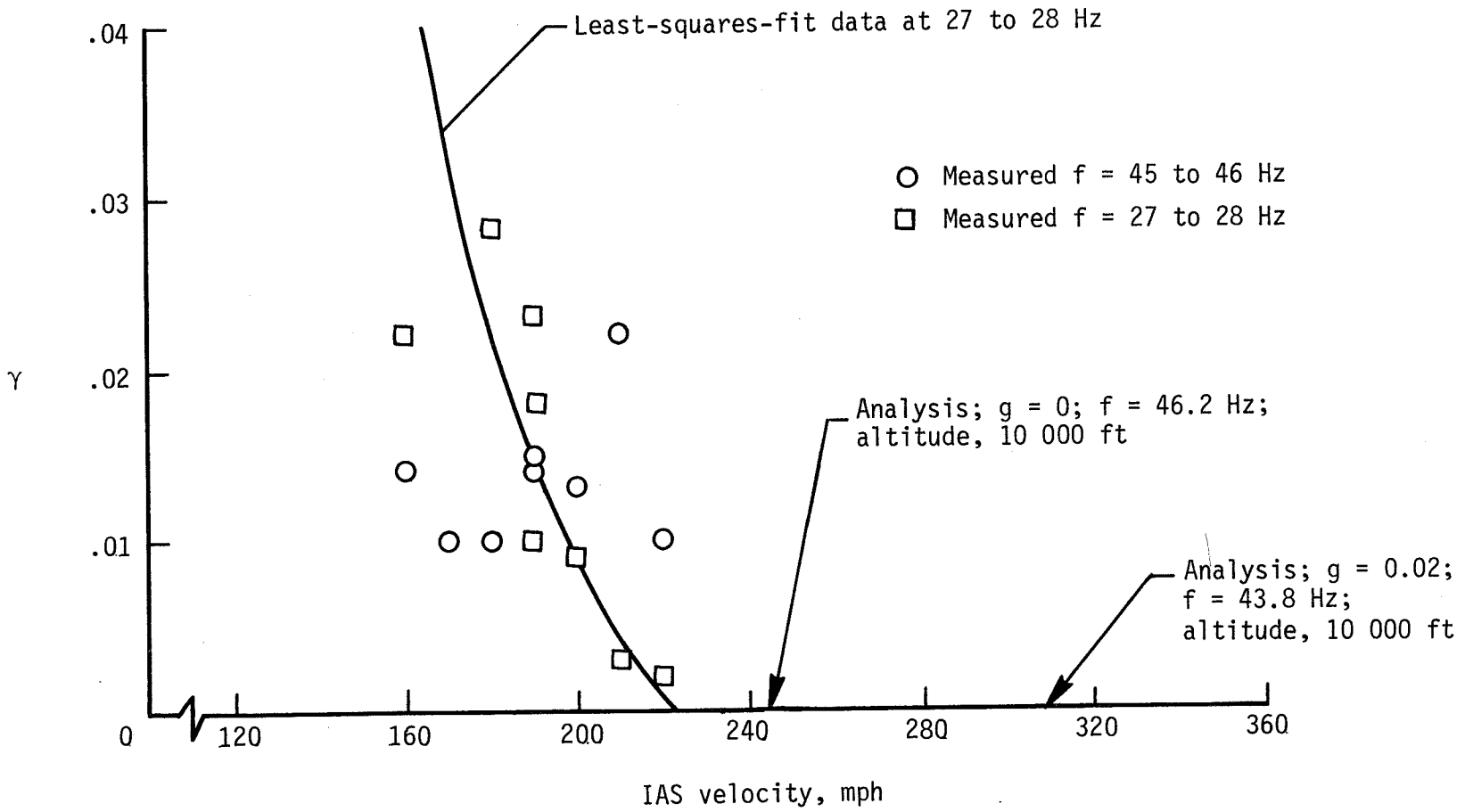

Figure 15.- Randomdec damping for response at two frequencies for the elevator accelerometer.

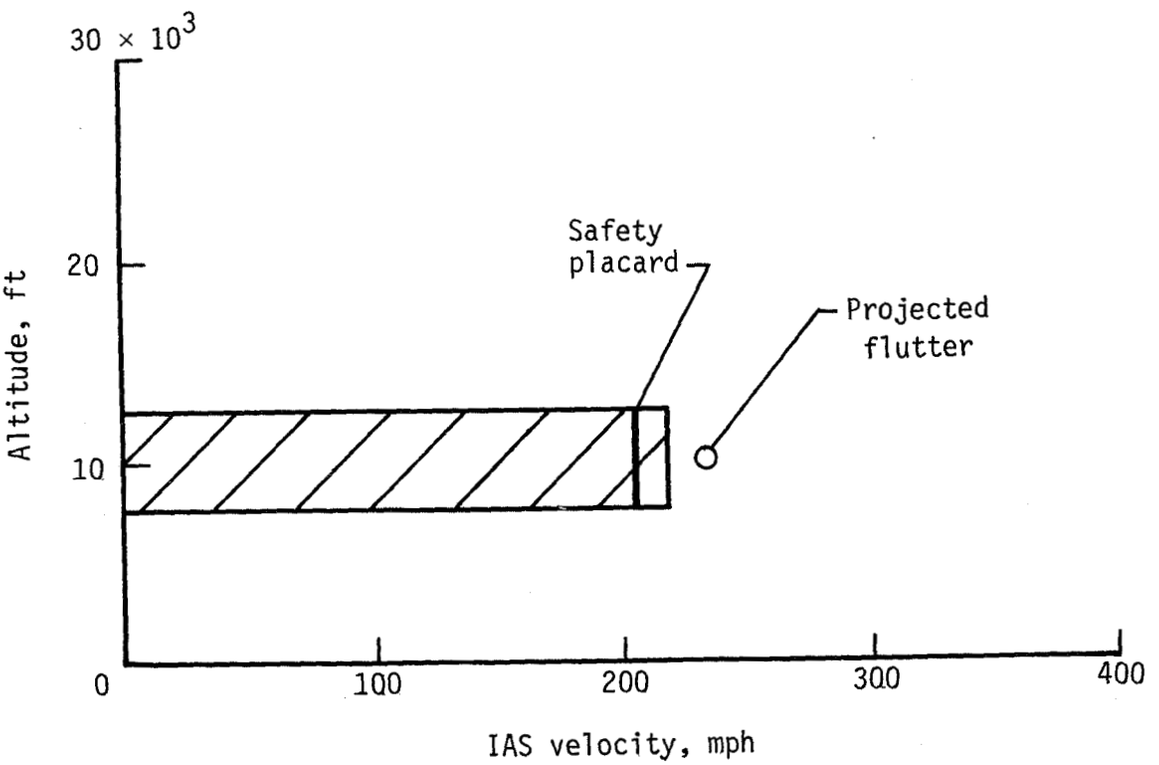

Figure 16.- Flight-test arena and safety placard for airplane operation.

1. Report No.	2. Government Accession No.	3. Recipient's Catalog No.
NASA TM-84528		

4. Title and Subtitle	5. Report Date
FLUTTER CLEARANCE OF THE HORIZONTAL TAIL OF THE BELLANCA SKYROCKET II AIRPLANE	September 1982
	6. Performing Organization Code 505-33-53-01
7. Author(s) Rodney H. Ricketts, F. W. Cazier, Jr., and Moses G. Farmer	8. Performing Organization Report No. L-15453
	10. Work Unit No.
9. Performing Organization Name and Address NASA Langley Research Center Hampton, VA 23665	11. Contract or Grant No.
	13. Type of Report and Period Covered Technical Memorandum
12. Sponsoring Agency Name and Address National Aeronautics and Space Administration Washington, DC 20546	14. Sponsoring Agency Code

15. Supplementary Notes

16. Abstract

The Skyrocket II is an all-composite-constructed experimental prototype airplane built by Bellanca Aircraft Engineering, Incorporated. A flutter-clearance program was conducted on the horizontal tail so that the airplane could be safely flown to acquire natural-laminar-flow aerodynamic data. Ground-vibration test data were used in a lifting-surface flutter analysis to predict symmetric and antisymmetric flutter boundaries. Subcritical-response data which were acquired during flight tests are compared with the analytical results. The final flutter-clearance placard speed was based on flight-test data.

17. Key Words (Suggested by Author(s))	18. Distribution Statement
Flight flutter test Aeroelasticity Subcritical response techniques Ground vibration test Flutter analysis	Unclassified - Unlimited Subject Category 05

19. Security Classif. (of this report)	20. Security Classif. (of this page)	21. No. of Pages	22. Price
Unclassified	Unclassified	48	A03

For sale by the National Technical Information Service, Springfield, Virginia 22161

NASA-Langley, 1982

National Aeronautics and
Space Administration

Washington, D.C.
20546

Official Business
Penalty for Private Use, $300

THIRD-CLASS BULK RATE

Postage and Fees Paid
National Aeronautics and
Space Administration
NASA-451

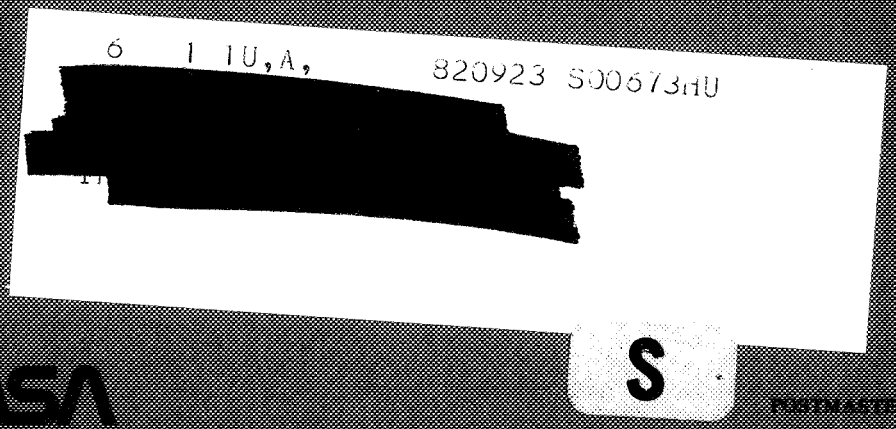

S

NASA

POSTMASTER: If Undeliverable (Section 158
Postal Manual) Do Not Return

Wilmington Univ.
OCT 29 1982
RECEIVED